Superior Charge Storage and Power Density of a Conducting Polymer-Modified Covalent Organic Framework

Catherine R. Mulzer, Luxi Shen, Ryan P. Bisbey, James R. McKone, Na Zhang, Héctor D. Abruña*, and William R. Dichtel*

Supplementary Information

Correspondence Addresses

Professor William R. Dichtel
Department of Chemistry
Northwestern University
Evanstion, IL 60208 (USA)
Tel: (+1)-847-467-6031
Email: wdichtel@northwestern.edu

Professor Héctor D. Abruña
Department of Chemistry and Chemical Biology
Cornell University
Baker Laboratory
Ithaca, NY 14853-1301 (USA)
Tel: (+1)-607-255-4720
Email: hda1@cornell.edu

Table of Contents

A. Materials and Instrumentation. All reagents were purchased from commercial sources and used without further purification. *N,N*-dimethylformamide was purchased from Sigma Aldrich and purified using a custom-built alumina column-based solvent purification system.

Infrared (IR) spectra were recorded on a Thermo Nicolet iS10 with a diamond ATR attachment or on a Bruker Vertex 80V with a Germanium ATR attachment and are uncorrected.

Grazing incidence X-ray diffraction (GIXD) was performed at the G2 station at Cornell High Energy Synchrotron Source (CHESS) using a beam energy of 11.25 ± 0.01 keV ($\lambda = 0.1103$ nm), selected using a single-crystal Be crystal monochromator. Motorized slits were used to define a 0.2 × 3 (V×H) mm^2 beam. The data were collected using a 640-element 1D diode-array, of which each element incorporates its own pulse counting electronics capable of count rates of ~105 photons s^{-1}. A set of 0.1° Soller slits were used on the detector arm to define the in-plane resolution. The scattering geometry is described in detail elsewhere.[1] Each data set was collected by scanning the detector with the sample stationary. The incidence angle, α, between the beam and sample surface was 0.340°. Axes labels $Q_\perp$ and $Q_{||}$ are defined using the GISAXS convention $Q_\perp = 4\pi/\lambda\sin(\delta/2)$ and $Q_{||} = 4\pi/\lambda\sin(\nu/2)$, where δ and ν are the vertical and horizontal scattering angles, respectively. At $\alpha=\delta=0$, $\hbar Q_{||}$ and $\hbar Q_\perp$ (where ħ is Planck's constant) are the components of momentum transfer parallel and perpendicular to the sample surface, respectively.

Atomic force micrographs (AFMs) were taken on an Asylum MFP-3D-BIO operating in tapping mode and equipped with a Tap300DLC diamond-like carbon or Tap150Al-G Si tip with aluminum reflex coating (tip composition was not seen to affect image quality).

X-ray photoelectron spectra (XPS) were taken using a Surface Science Instruments SSX-100 system with operating pressure ~$2x10^{-9}$ Torr. Monochromatic AlK-alpha x rays (1486.6 eV) were used with beam diameter of 1 mm. Photoelectrons were collected at a 55 ^{o} emission angle. A

hemispherical analyzer determined electron kinetic energy, using a pass energy of 150 V for wide/survey scans, and 50 V for high resolution scans. A flood gun was used for charge neutralization of non-conductive samples.

Surface area measurements were conducted on a Micromeritics ASAP 2020 Accelerated Surface Area and Porosimetry Analyzer using eight 1 μm thick **DAAQ-TFP** COF films. Samples were degassed at 80 °C for 2 hours. Krypton isotherms were generated by incremental exposure to ultra high purity krypton up to P/P_0 of 0.4 over 12-hour periods in a liquid nitrogen (77K) bath. Surface parameters were determined using BET adsorption models (Micromeritics ASAP 2020 V1.05).

Electrochemical-Quartz Crystal Microbalance (EQCM) experiments were performed using a Stanford Research Systems QCM 200 interfaced to a Princeton Applied Research Versastat3 potentiostat. **DAAQ-TFP** COF was grown on O100RX3 quartz resonators (Au with Ti adhesion layer) using the slow addition method described below. A water-jacketed beaker was used to maintain a constant temperature of 25 °C during the EQCM experiment. The changes in mass and resistance were monitored over the experimental time. A 100 mL solution of 0.1 M EDOT in a 0.1 M tetrabutylammonium perchlorate (TBAP)/MeCN supporting electrolyte was used for the electropolymerization with a carbon counter electrode. Potentials were referenced to a $Ag/AgClO_4$ reference electrode.

Electrochemistry experiments were conducted on a Princeton Applied Research VersaSTAT 3 potentiostat using a standard three electrode cell configuration, a 27 gauge Pt wired coiled or high surface area carbon as the counter electrode, and either an aqueous Ag/AgCl or organic $Ag/AgClO_4$ (standardized against Fc/Fc^+) reference electrode. For the 0.5 M H_2SO_4, milliQ purified water was used. The 0.1 M TBAP supporting electrolyte was prepared using

electrochemistry grade tetrabutylammonium perchlorate that was recrystallized from ethyl acetate, and anhydrous acetonitrile (Sigma Aldrich), which was stored over activated 3 Å sieves..

B. Synthetic Procedures

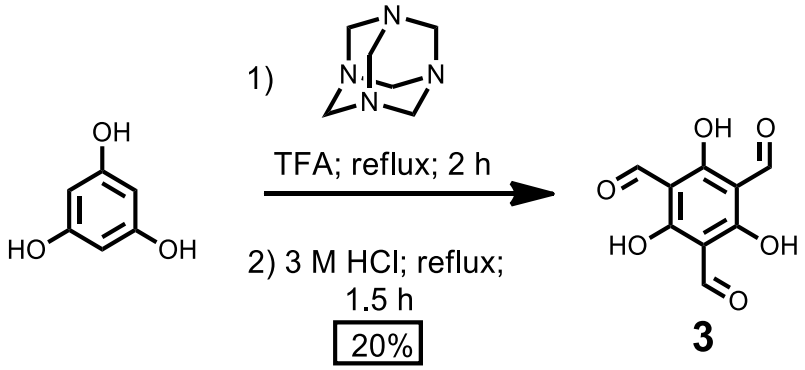

Synthesis of 1,3,5-triformylphloroglucinol, TFP: TFP was synthesized following previously reported procedure and characterization matched that in the literature.[2]

Synthesis of DAAQ-TFP Films:

Crystalline film growth: To a glass vial, a **DAAQ** (17 mg, 0.071 mmol) in *N*,*N*-dimethylformamide was added. A gold electrode (2.5 cm x 1.3 cm) was submerged in the solution and a septum cap placed on the top of the vial. The solution was placed on a preheated 90 °C hotplate. Subsequently, **TFP** (10 mg, 0.048 mmol) was added over the course of one hour via syringe from a 10 mg mL^{-1} solution in DMF. During the course of the addition, the reaction mixture was gently swirled. After the addition the reaction was allowed to heat at 90 °C for an additional 3 hours. The total reaction time was 4 hours (including **TFP** addition) and final volume was 4.2 mL (after **TFP** addition).

Electropolymerization of 3,4-ethylenedioxythiophene (EDOT): The electropolymerization was performed in a standard three-electrode configuration under an Ar atmosphere. The cell

consisted of a **DAAQ-TFP** COF film on gold (prepared as described above) as the working electrode, a $Ag/AgClO_4$ reference electrode, and either a coiled Pt wire or high surface area carbon counter electrode. A controlled area (0.64 cm^2) surface cell was used for electrochemistry experiments. A 0.1 M solution of EDOT was prepared in 0.1 M TBAP, and nine electropolymerization cycles between -0.5 and 1.1 V vs $Ag/AgClO_4$ at 20 mV s^{-1} were performed. A nine-cycle polymerization passes the oxidative potential 10 times, because the initial cycle starts from open circuit, which is approximately 0.2 V vs $Ag/AgClO_4$. The counter electrode was placed in the same location relative to the working electrode during electropolymerization (c.a. 2 cm separation). After electropolymerization, the working electrode was rinsed three times with acetonitrile and two times with acetone prior to its electrochemical testing.

C. Atomic Force Microscopy (AFM)

AFM images were processed using Gwyddion 2.34 software. The image was leveled, such that the exposed substrate surface was flat as shown by the height profiles below. Heights were calculated using an areal mask over the film surfaces. Step edges were achieved by scratching the **DAAQ-TFP** / PEDOT composite carefully so as to avoid scratching the underlying gold surface. On each film, three locations were analyzed and then averaged to give the film height. The height profiles displayed below demonstrate that a clean step edge was obtained and that the film was leveled appropriately.

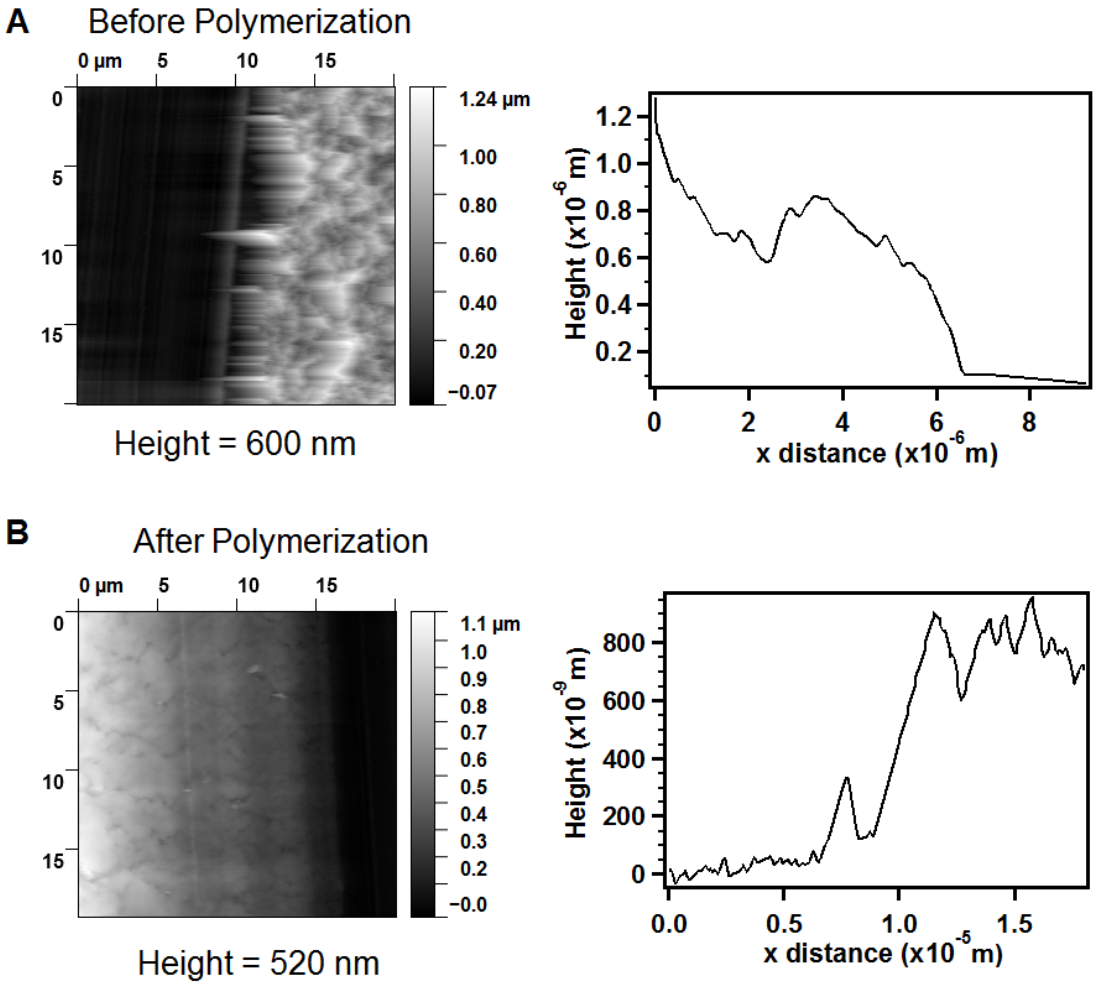

Figure S1. Representative AFMs of crystalline **DAAQ-TFP** COF films (A) before EDOT polymerization and (B) after EDOT polymerization.

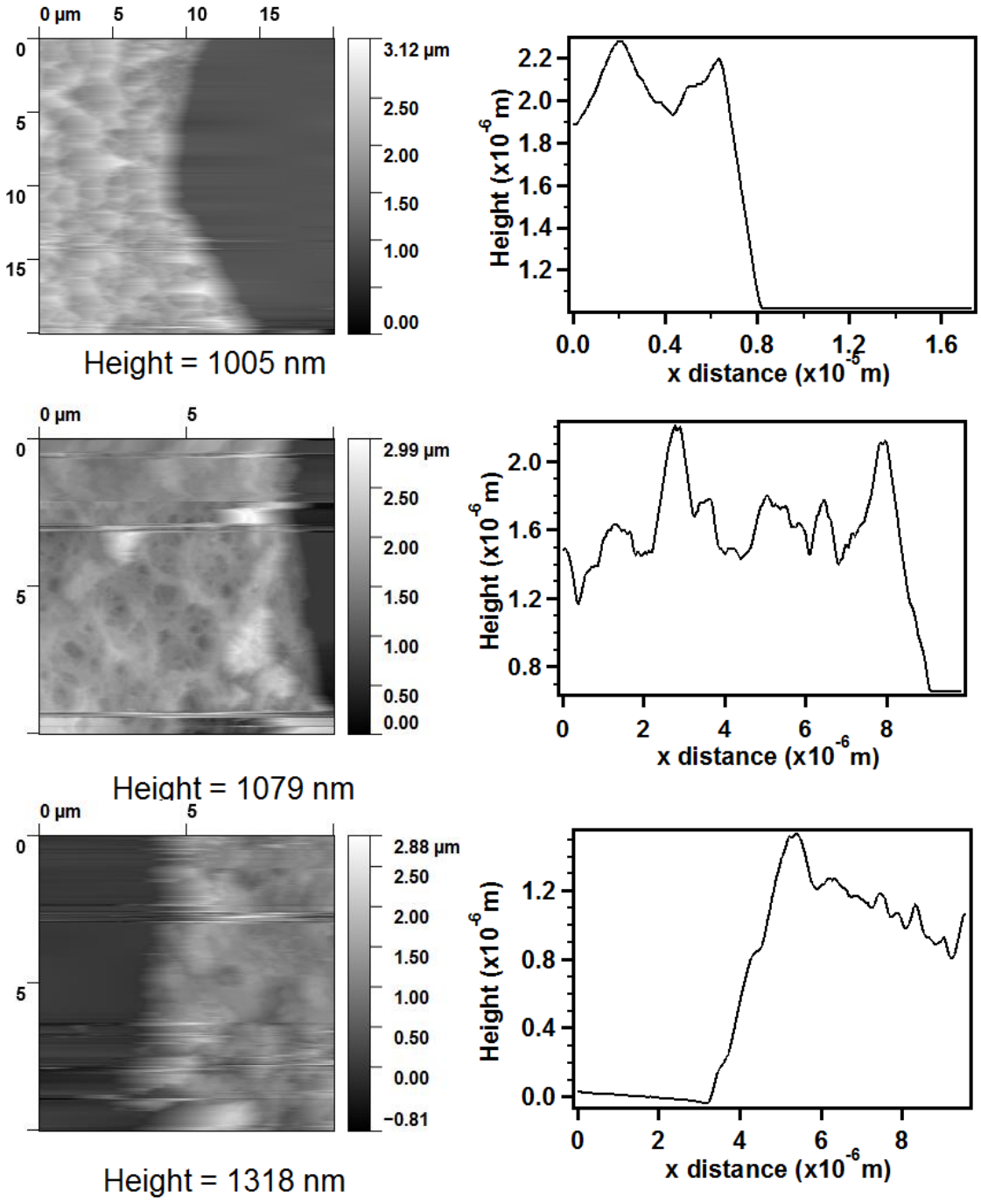

Figure S2. Representative AFMs of the thickest crystalline **DAAQ-TFP** COF films (approximately 1 µm).

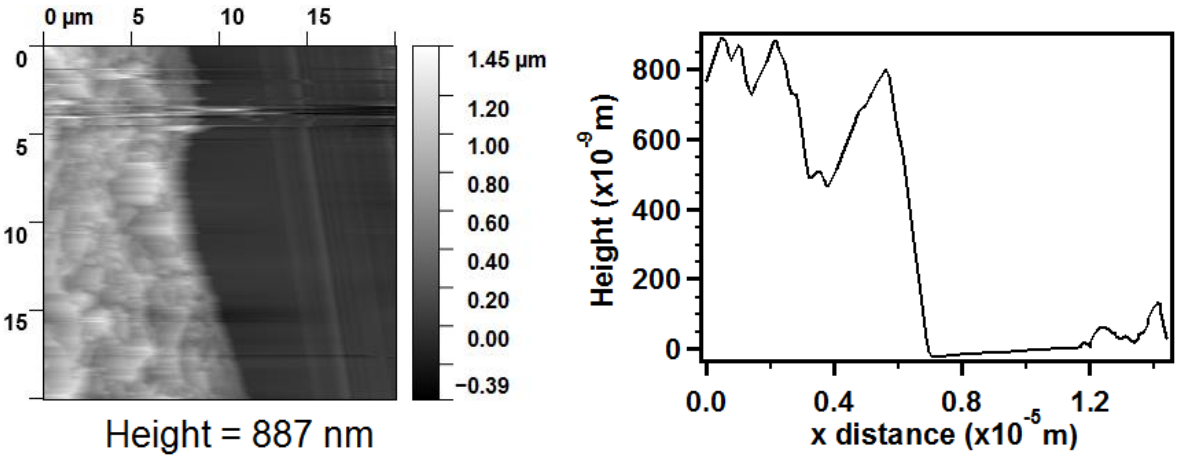

Figure S3. Representative AFM PEDOT-modified Au AFMs for a polymerization to yield approximately 805 nm thick film for control experiments.

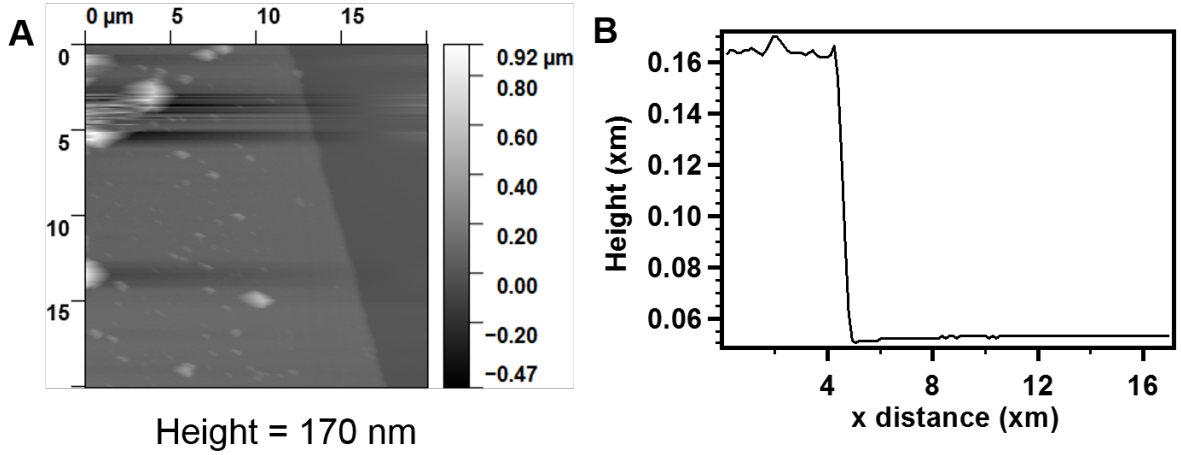

Figure S4. Representative AFMs of a PEDOT-modified **DAB-TFP** COF film on Au.

D. Scanning Electron Microscopy (SEM)

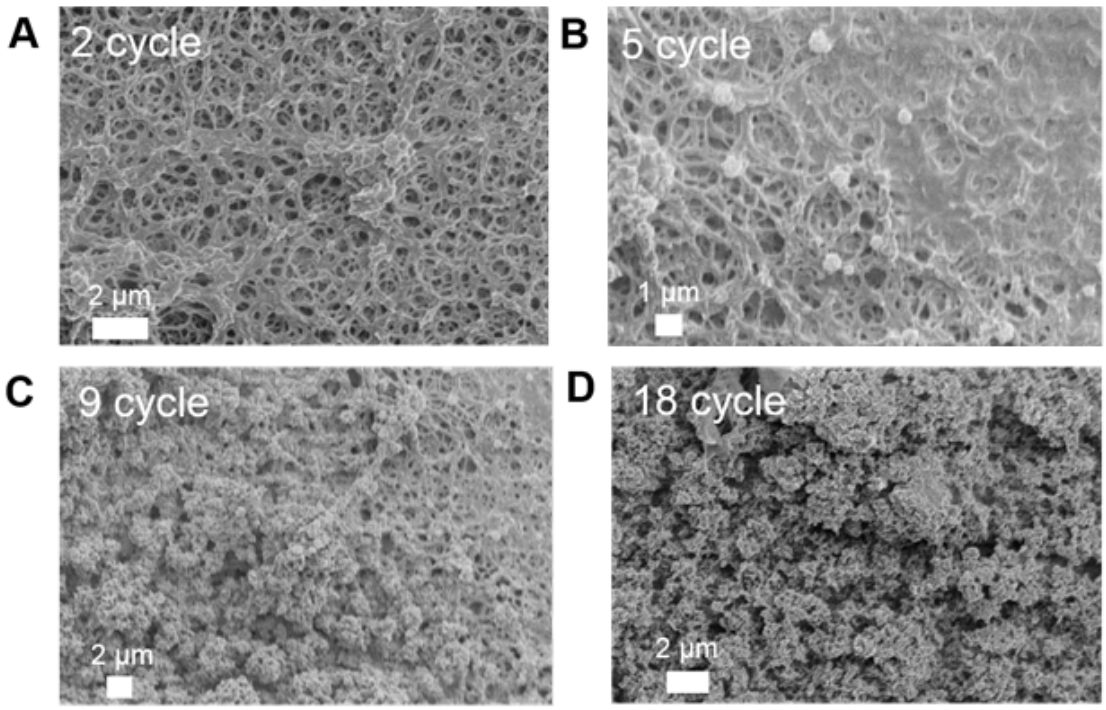

Figure S5. Representative SEMs of post-polymerization **DAAQ-TFP** COF films after polymerization for (A) 2 cycles, (B) 5 cycles, (C) 9 cycles, and (D) 18 cycles.

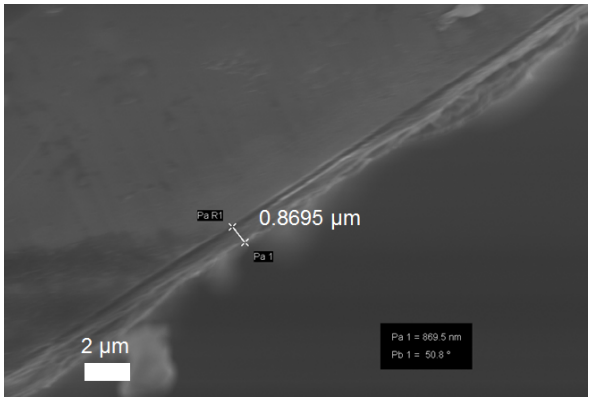

Figure S6. Cross sectional SEM of post-polymerization **DAAQ-TFP** COF film after 9 polymerization cycles.

E. Grazing Incidence Diffraction (GIXD)

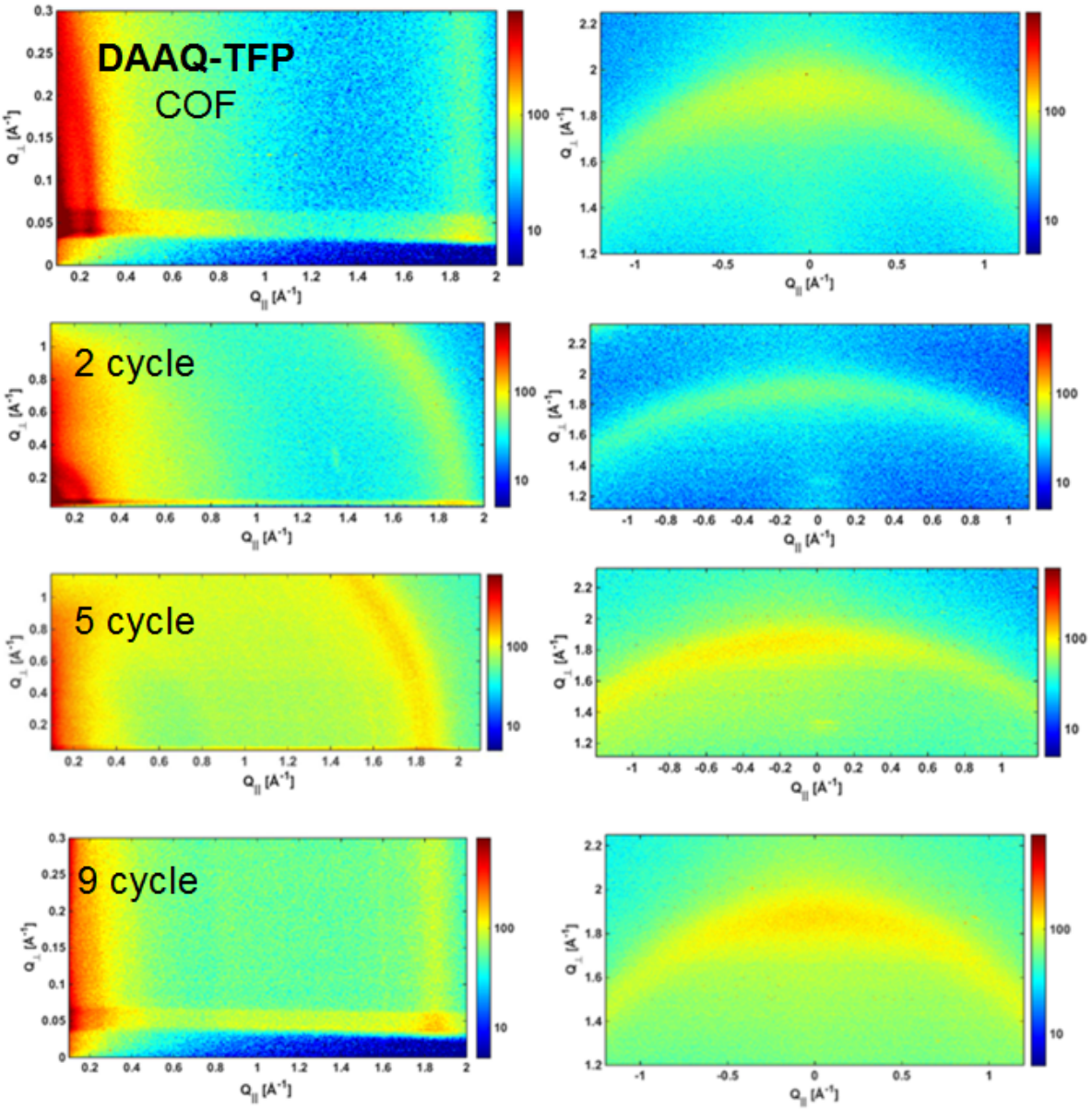

Figure S7. Representative GIXD of **DAAQ-TFP** films on Au substrates. The top row corresponds to a **DAAQ-TFP** COF film prior to electropolymerization. Subsequent rows correspond to 2, 5, and 9 electropolymerization cycles, respectively.

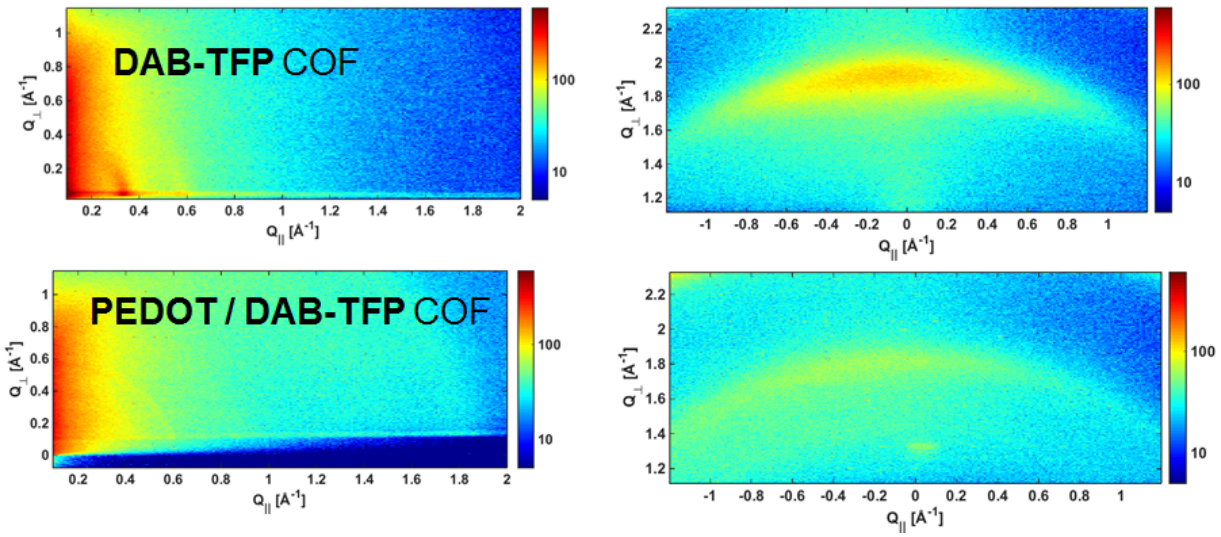

Figure S8. Representative GIXD **DAB-TFP** films on Au substrates.

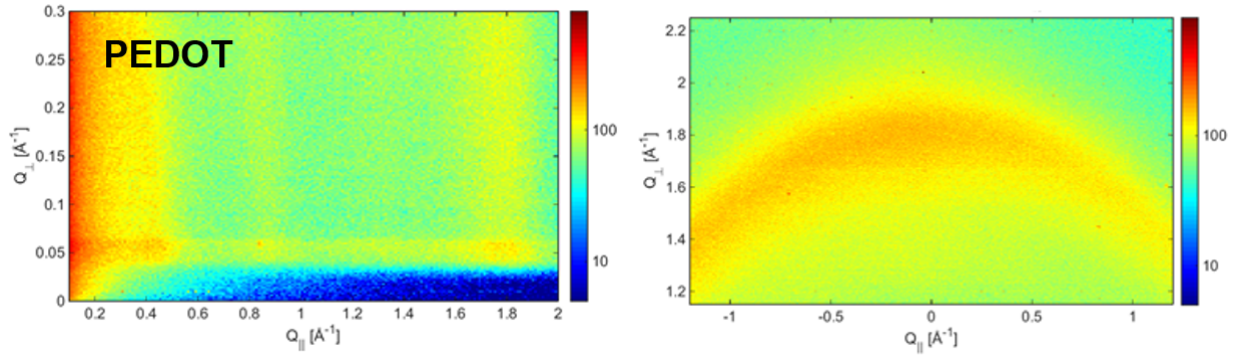

Figure S9. GIXD of PEDOT polymerized on Au substrate.

F. Quartz Crystal Microbalance (QCM)

The Sauerbrey mass of the electrodeposited PEDOT was calculated using the Sauerbrey equation $\left(\Delta f = \frac{2f_0^2}{A(\rho_q \mu_q)^{\frac{1}{2}}} \Delta m\right)$ where Δf is the frequency change, f_0 is the resonant frequency, Δm is the change in mass, A is the piezoelectric active area, ρ_q is the density of quartz, and μ_q is the shear modulus of the quartz. During the electropolymerization of EDOT, there is a linear increase in Sauerbrey mass accompanied by a corresponding linear increase in resistance. This resistance increase indicates that viscoelastic losses increase during the electropolymerization, such that the Sauerbrey mass represents an upper limit of the deposited gravimetric mass of the PEDOT. We find that the change in frequency for a given resistance change is roughly identical for each cycle, such that the overestimated mass is still proportional to the actual mass throughout the electropolymerization.

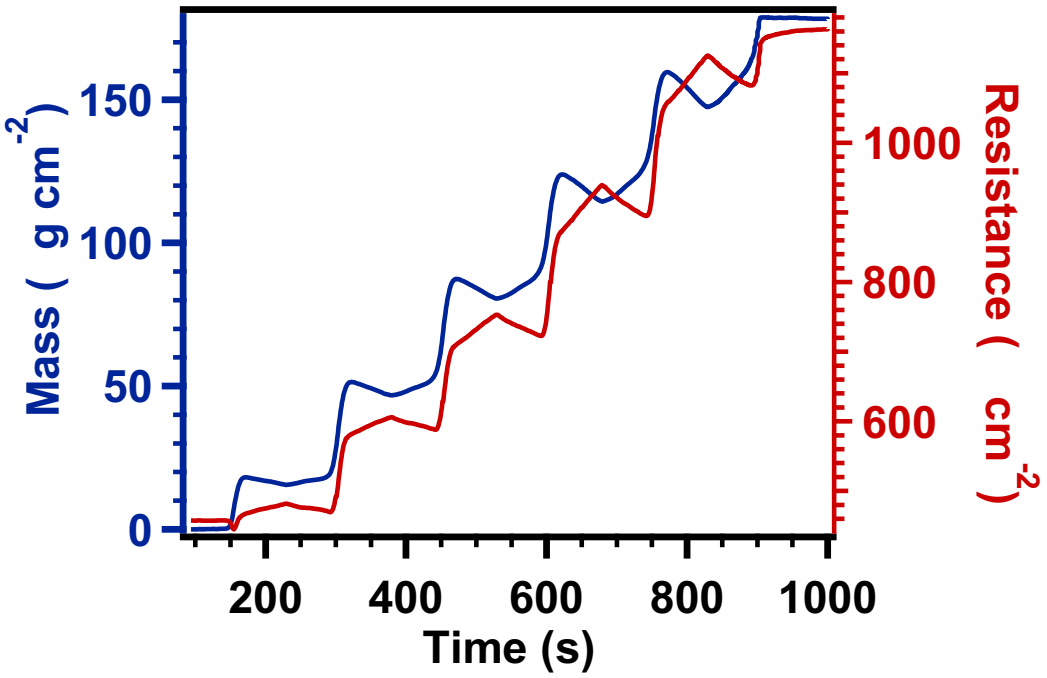

Figure S10. Mass (blue) and resistance (red) change for EQCM polymerization of EDOT within **DAAQ-TFP** on QCM chip.

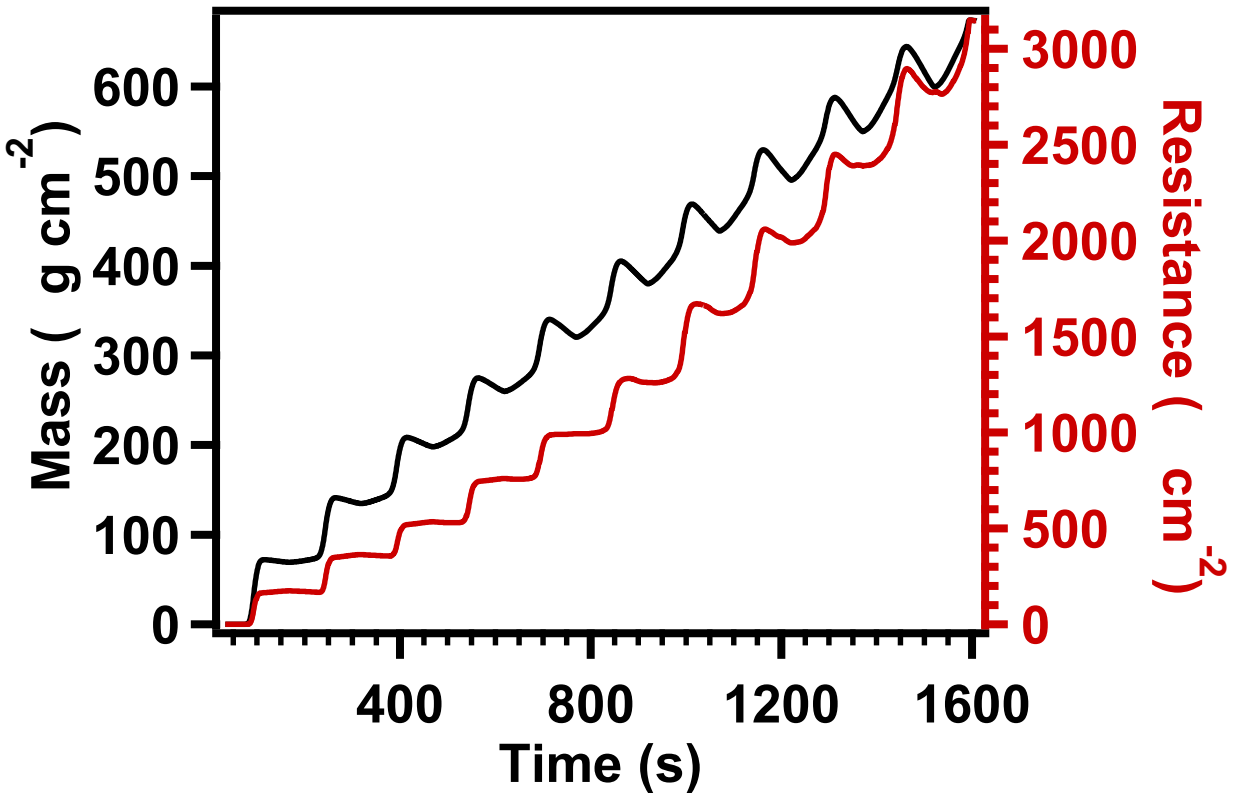

Figure S11. Recorded mass (black) and resistance (red) change over time with EQCM electropolymerization of EDOT on bare Au.

G. Surface Area Analysis

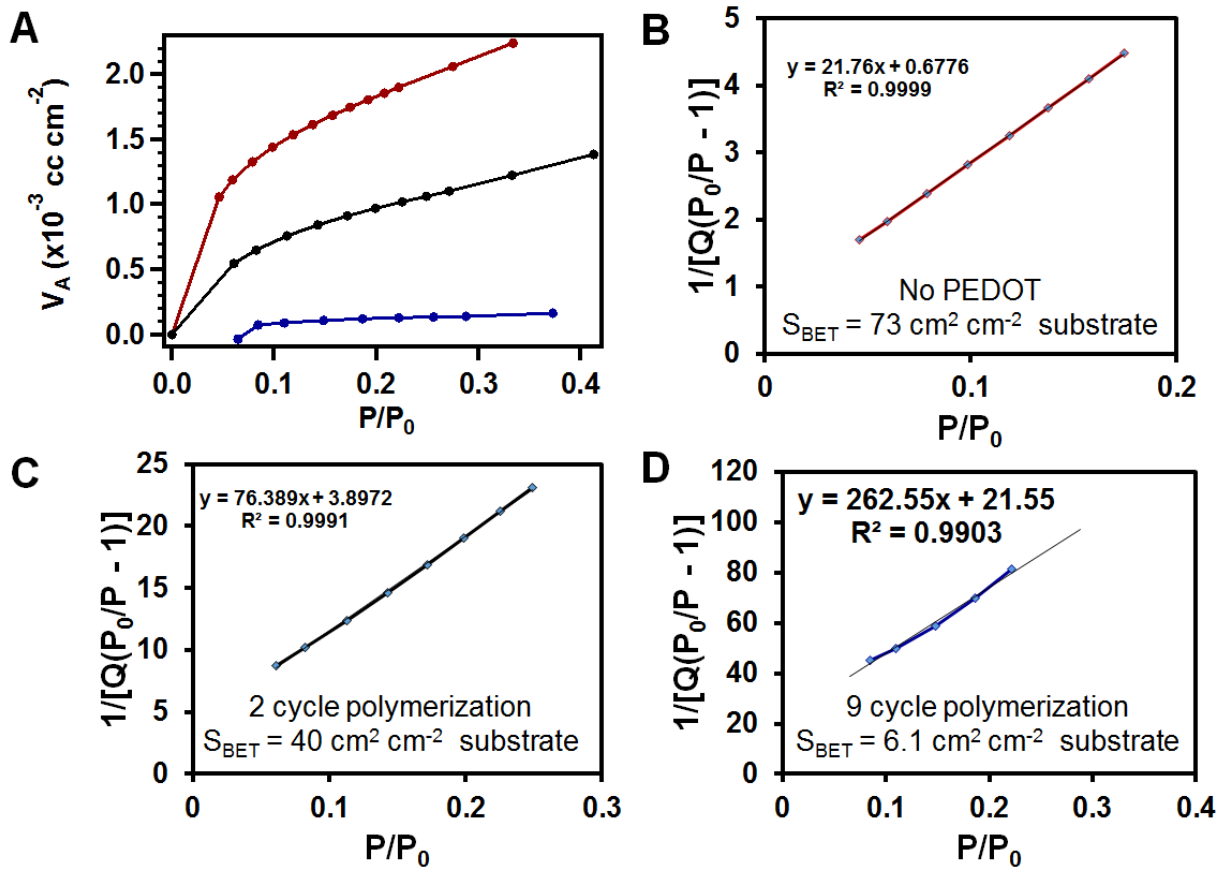

Figure S12. (A) Kr gas adsorption isotherm for **DAAQ-TFP** COF without PEDOT (red), 2 cycle polymerization PEDOT / **DAAQ-TFP** COF (black), and 9 cycle polymerization PEDOT / **DAAQ-TFP** COF (blue). BET transforms for (B) **DAAQ-TFP** COF without PEDOT, (C) 2 cycle polymerization PEDOT / **DAAQ-TFP** COF, and (D) 9 cycle polymerization PEDOT / **DAAQ-TFP** COF.

H. Electrochemical Methods and Data

Analyses were performed in a standard three electrode set up: a **DAAQ-TFP** film modified gold substrate, a Ag/AgCl or a $Ag/AgClO_4$ reference, and a coiled Pt wire or high surface area carbon counter. All experiments were performed after purging the electrolyte with argon. Electropolymerization was carried out using 0.1 M EDOT in 0.1 M TBAP / MeCN *via* cyclic voltammetry (CV) between -0.5 and 1.0 V vs $Ag/AgClO_4$. The composite films were studied in 0.5 M H_2SO_4.

Electropolymerization was optimized at nine cycles (20 mV s^{-1}, 0.1 M EDOT / 0.1 M TBAP / MeCN, Figures S14 and S15). When the electropolymerization was carried out for two or five cycles, the amount of charged stored in the films was less than the theoretical (assessed through integration of the anthraquinone oxidation peak). When an 18 cycle polymerization was tested, the amount of charge stored in the film diminished with increased scan rate indicating poor access to the anthraquinones. This is consistent with densely polymerizing and overloading the COF with PEDOT such that electrolyte and counter ions cannot "keep up" with the redox-processes at the higher scan rates. This is seen in the light blue CV response in Figure S14 where the peaks associated with the anthraquinones are no longer well defined above PEDOT background. When EDOT is polymerized at a slower scan rate (2 mV s^{-1}, Figure S15) we also see poorly defined redox waves with an overall resistive response again consistent with "overly dense" PEDOT within the COF pores.

Approximation of Quinones Accessed in films (sample calculations)

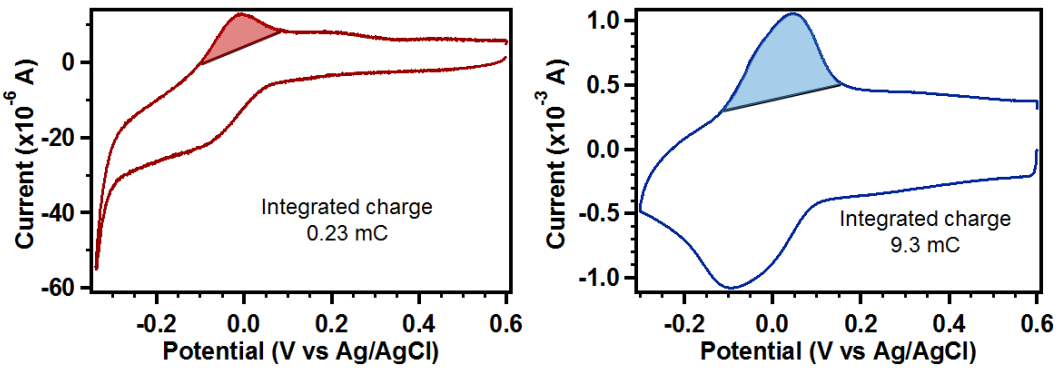

Figure S13. Sample CVs used to approximate the number of anthraquinones accessed in PEDOT-modified **DAAQ-TFP** COF films. The left CV shows an unmodified **DAAQ-TFP** COF film and the right shows a PEDOT-modified **DAAQ-TFP** COF film.

(1) Determine unit cells of **DAAQ-TFP** COF exposed in the electrochemistry cell.

Unit cell area: 770 Å^2

Exposed geometric area in echem cell: 0.64 cm^2

Number of unit cells in echem cell: $\frac{6.4 \times 10^{-5}\ \mathrm{m^2}}{7.7 \times 10^{-18}\ \mathrm{m^2}} = 8.3 \times 10^{12}$ unit cells

(2) Each unit cell provides one anthraquinone, so 8.3×10^{12} quinones are exposed providing 1.6×10^{13} electrons or 2.7×10^{-11} moles of electrons

(3) Each mole of electron gives 96485 C. Therefore, each layer will provide 2.7×10^{-11} moles $\left(96485\ \frac{\mathrm{C}}{\mathrm{mole}}\right) = 2.7 \times 10^{-6}$ C

(4) Convert this charge to charge per nm

$$\left(2.7 \times 10^{-6}\ \frac{\mathrm{C}}{\mathrm{layer}}\right)\left(0.362\ \frac{\mathrm{nm}}{\mathrm{layer}}\right)^{-1} = 7.4\ \frac{\mu\,\mathrm{C}}{\mathrm{nm}}$$

(5) From AFM determine the thickess. For Figure 3 in the text, film thickness of 1300 nm.

(6) Multiply by the charge per nm to get theoretical percent of anthraquinones

$$7.4\ \frac{\mu\ \mathrm{C}}{\mathrm{nm}}\ (1300\ \mathrm{nm}) = 9.6\ \mathrm{mC}$$

(7) Ratio the integrated oxidation charge from Figure S26 to the theoretical charge.

$$\left(\frac{0.23\ \mathrm{mC}}{9.6\ \mathrm{mC}}\right)100 = 3\%\ \left(\frac{9.3\ \mathrm{mC}}{9.6\ \mathrm{mC}}\right)100 = 97\%$$

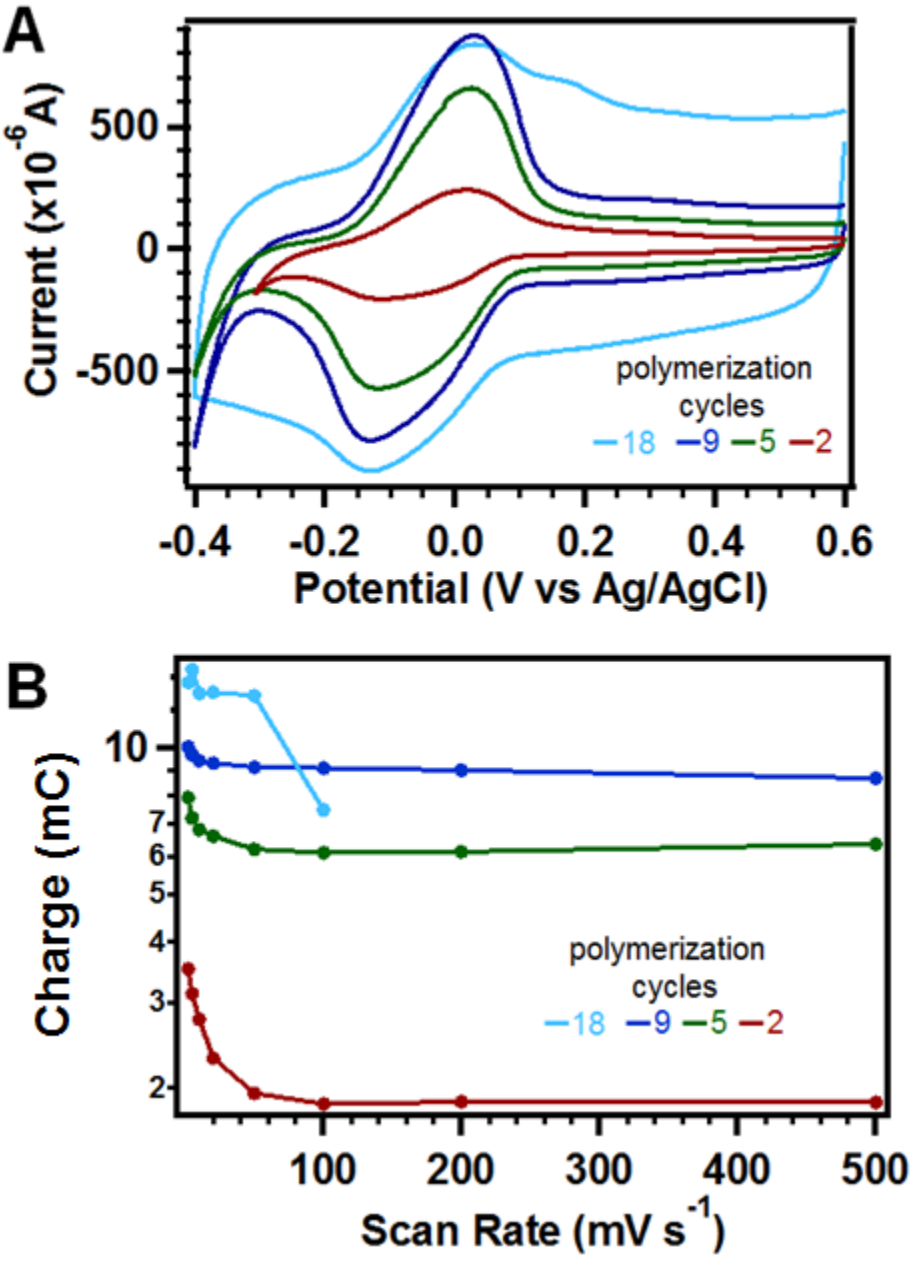

Figure S14. Effect of number of cycles in EDOT polymerization on **DAAQ-TFP** COF electrochemical response where line colors correspond to various number of cycles in the electropolymerization as designated on the above figures. (A) Cyclic voltammetric response of composite films in 0.5 M H_2SO_4, 20 mV s^{-1}. (B) Charge stored over a variety of scan rates.

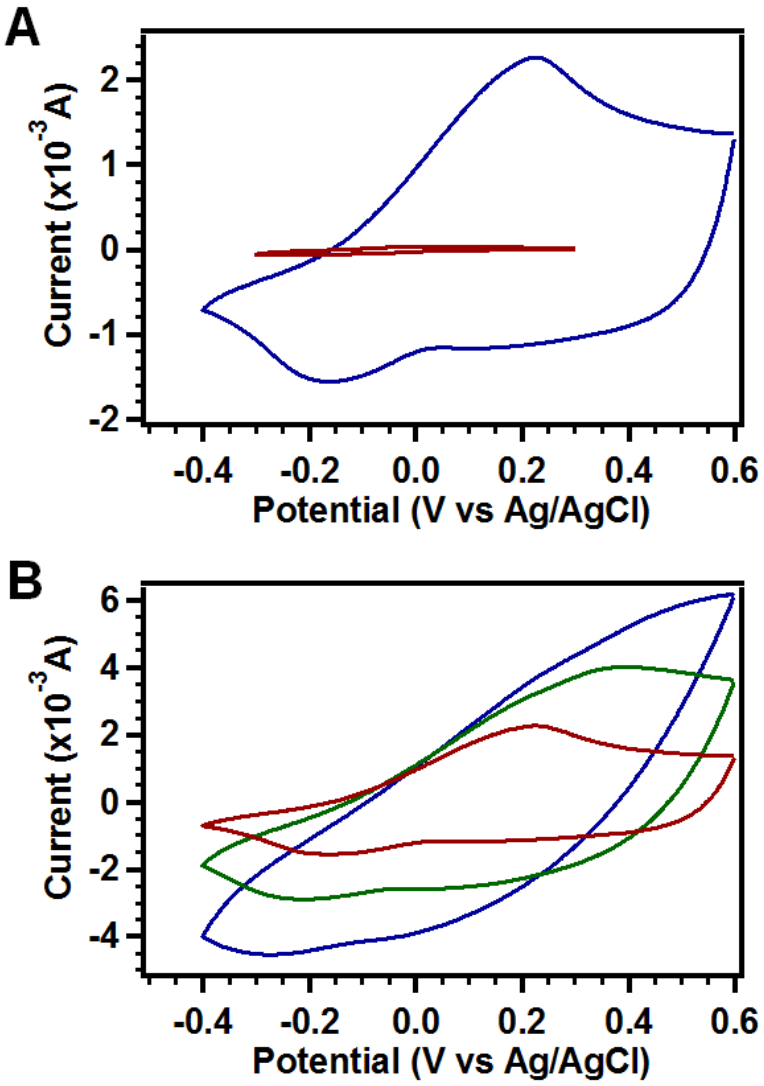

Figure S15. Effect of electropolymerization scan rate. (A) Cyclic voltammograms for unmodified **DAAQ-TFP** COF (red) and PEDOT / **DAAQ-TFP** COF where the PEDOT was polymerized at 2 mV s^{-1} for 5 cycles. CVs taken at 20 mV s^{-1} in 0.5 M H_2SO_4. (B) Scan rate dependence of film prepared in Figure S15A at 20 mV s^{-1} (red), 50 mV s^{-1} (green), and 100 mV s^{-1}.

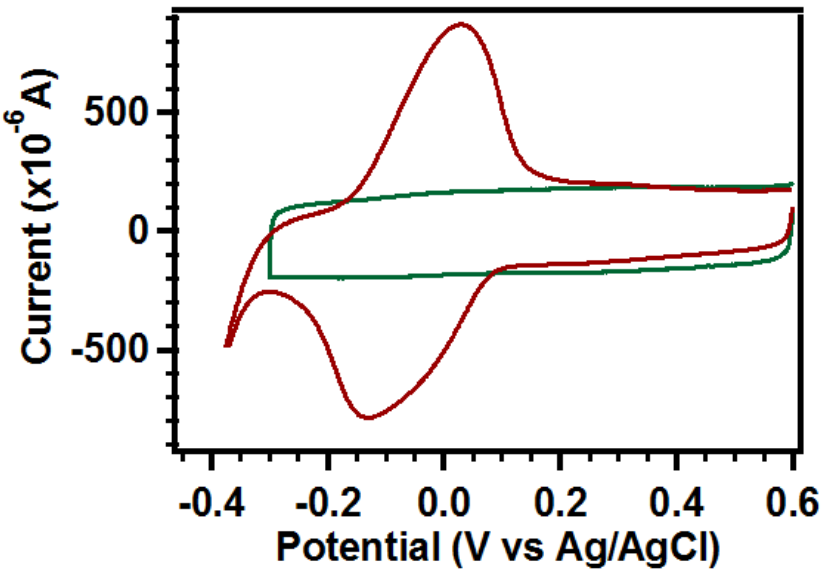

Figure S16. Overlay of cyclic voltammograms (20 mV s^{-1}, 0.5 M H_2SO_4) for PEDOT / **DAAQ-TFP** COF(red), and PEDOT / Au (green).

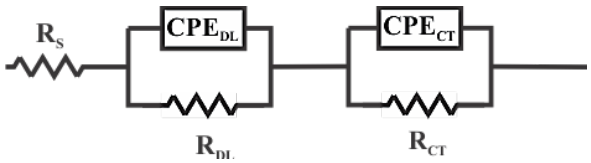

Figure S17. Equivalent circuit modeling for PEDOT / **DAAQ-TFP systems**

Table S1. Fitting parameters for PEDOT / **DAAQ-TFP** COF and **DAAQ-TFP** COF.

Substrate	**R_s (Ω)**	**E_s (Ω)**	**R_{DL} (Ω)**	**E_{RDL} (Ω)**	**CPE_{DL} (mF)**	**E_{DL} (mF)**	**R_{CT} (Ω)**	**E_{RCT} (Ω)**	**CPE_{CT} (mF)**	**E_{CT} (mF)**
PEDOT-modified **DAAQ-TFP** COF	19.7	0.32	22	0.17	400	0.01	21336	4547	4.7	0.023
unmodified **DAAQ-TFP** COF	451.6	1.89	1696	338	0.053	0.0039	9976	5110	0.13	0.018

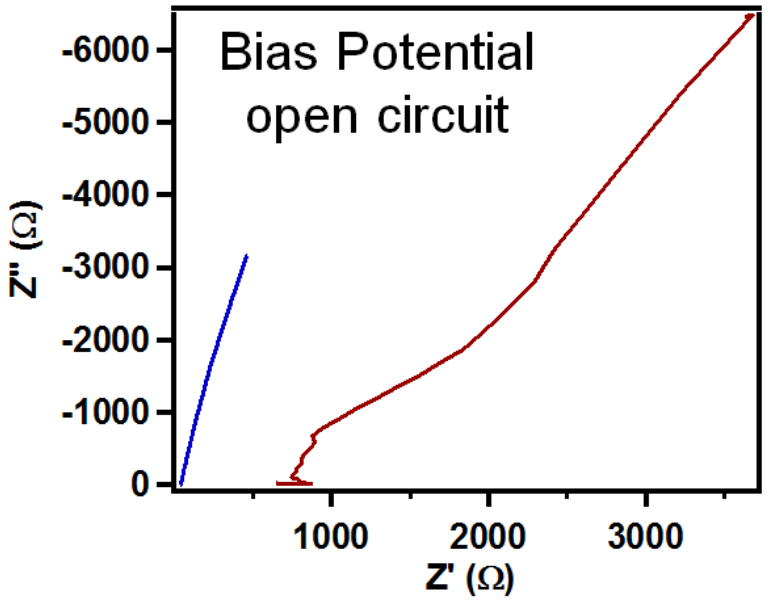

Figure S18. Impedance spectra comparing PEDOT / **DAAQ-TFP** (blue) and **DAAQ-TFP** COF (red).

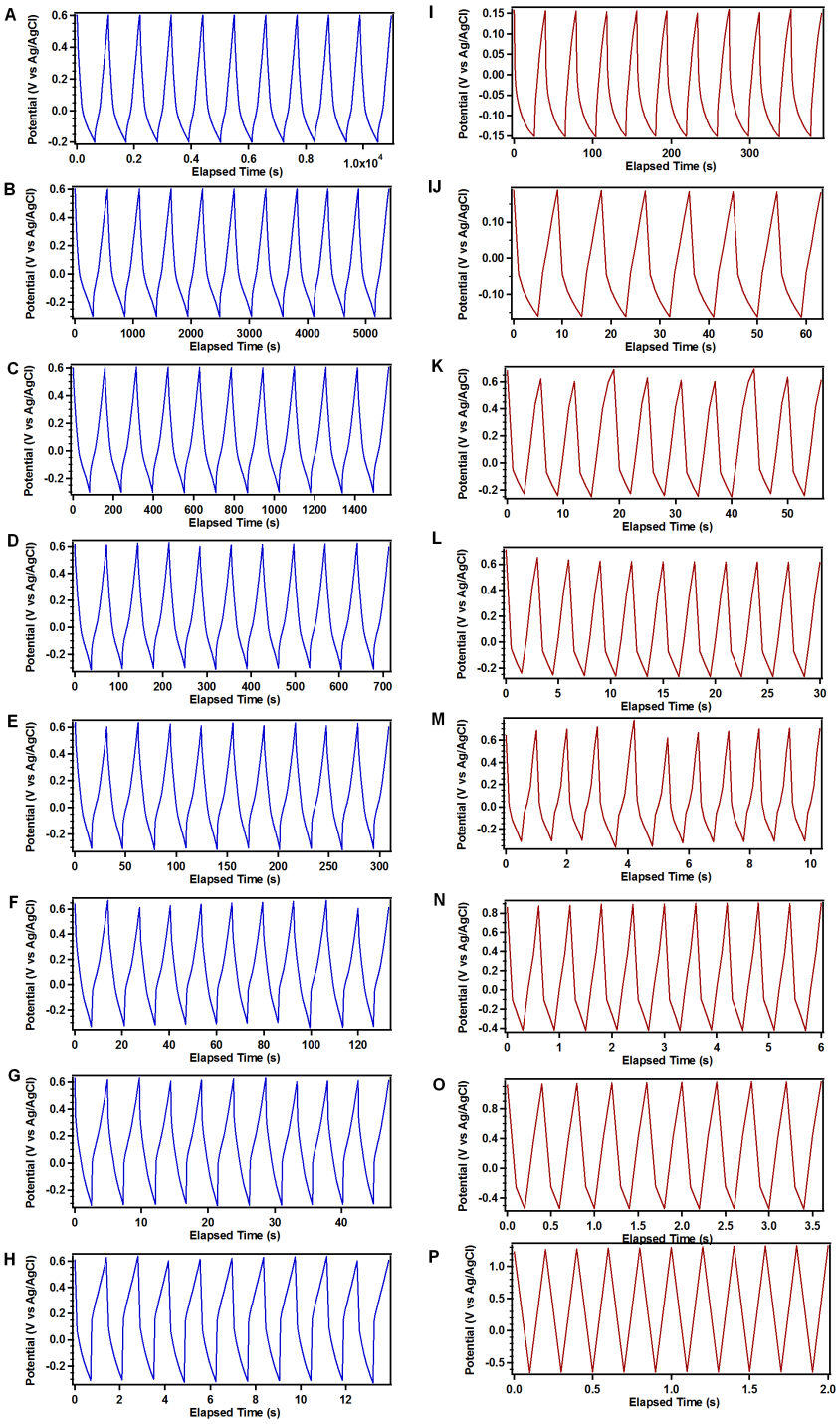

Figure S19. Galvanostatic charge discharge profiles over 10 cycles for PEDOT / **DAAQ-TFP** COF (A) 10C, (B) 20C, (C) 50C, (D) 100C, (E) 200C, (F) 400C, (G) 800C, (H) 1600C and **DAAQ-TFP** COF (I) 10C, (J) 20C, (K) 50C, (L) 100C, (M) 200C, (N) 400C, (O) 800C, (P) 1600C.

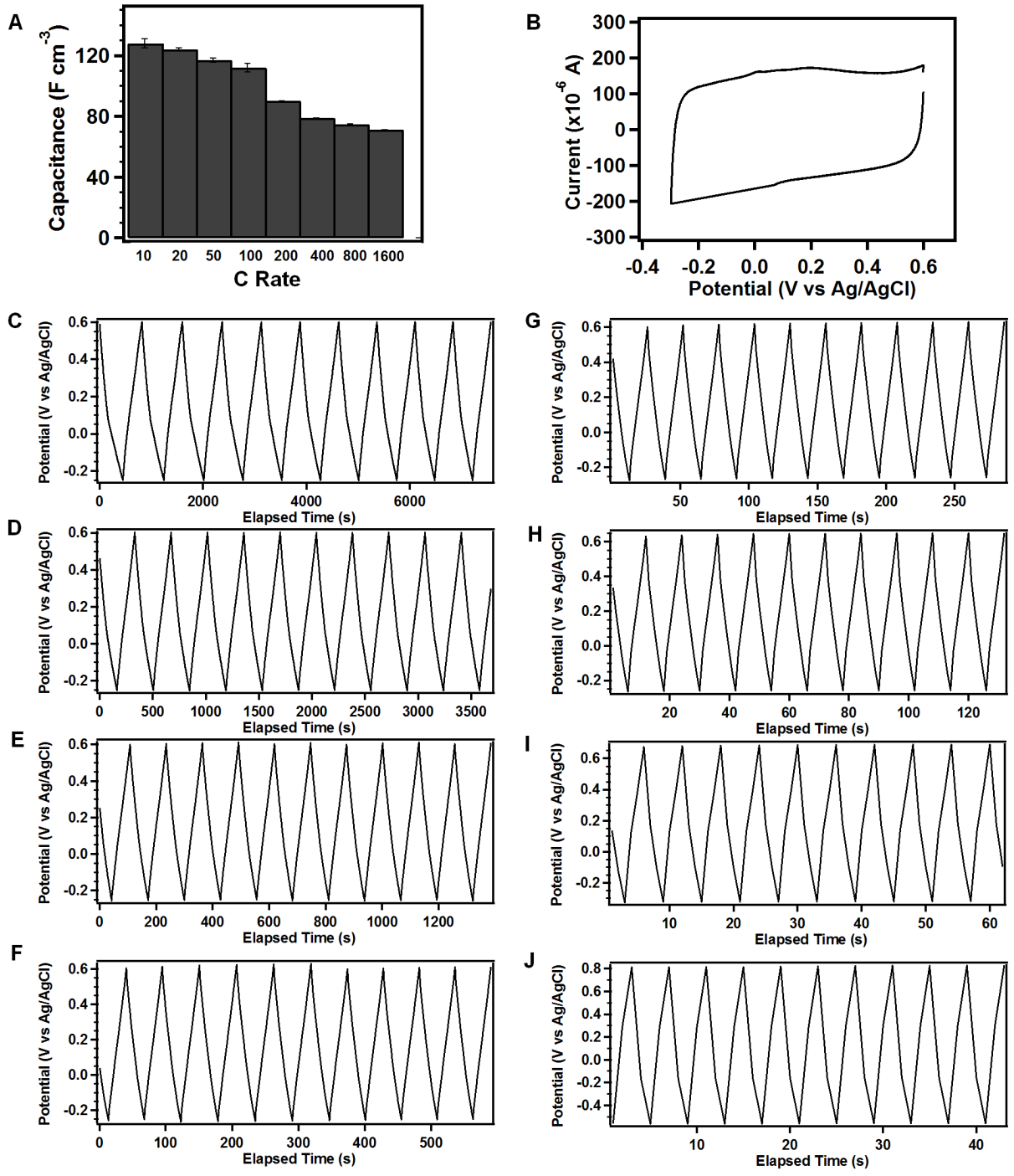

Figure S20. (A) Volumetric capacitances obtained from PEDOT on gold control experiment. (B) CV of PEDOT which has been electropolymerized from EDOT on Au substrate without COF present. The CV is taken in 0.5 M H_2SO_4 at 20 mV s^{-1}. (C) Galvanostatic charge discharge profiles over 10 cycles for PEDOT / Au (D) 10C, (E) 20C, (F) 50C, (G) 100C, (H) 200C, (I) 400C, (J) 800C.

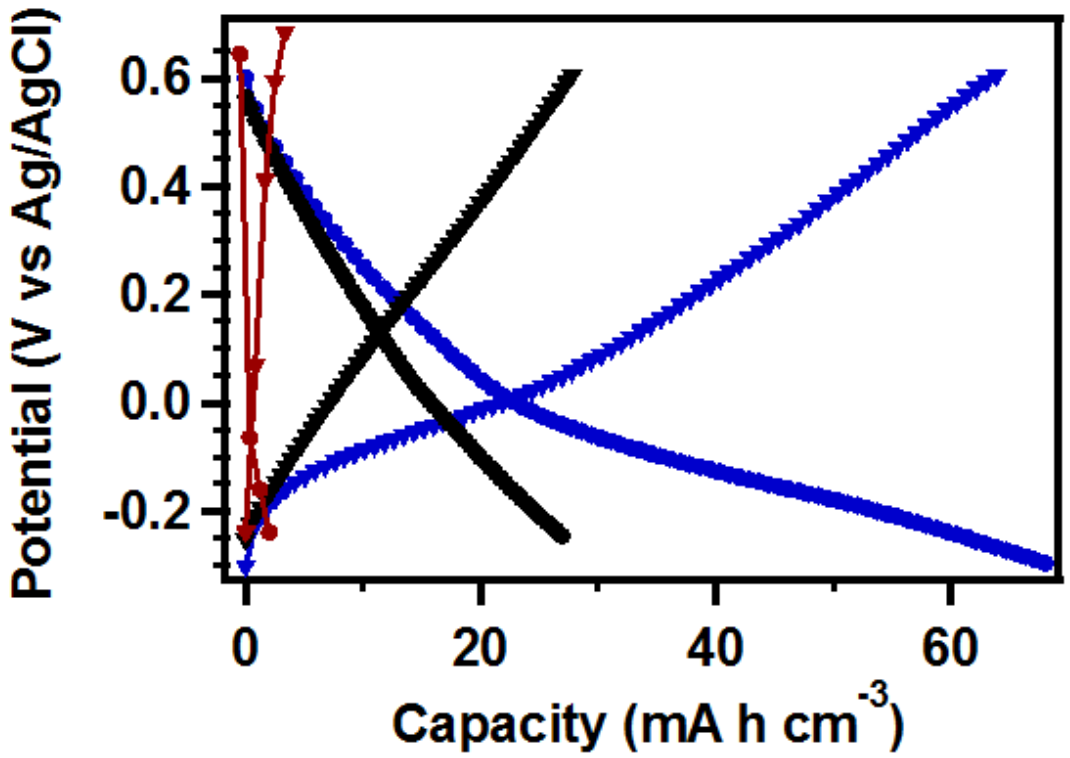

Figure S21. Potential / Capacity profiles for **DAAQ-TFP** COF (red), PEDOT / **DAAQ-TFP** COF (blue), and PEDOT / Au (black).

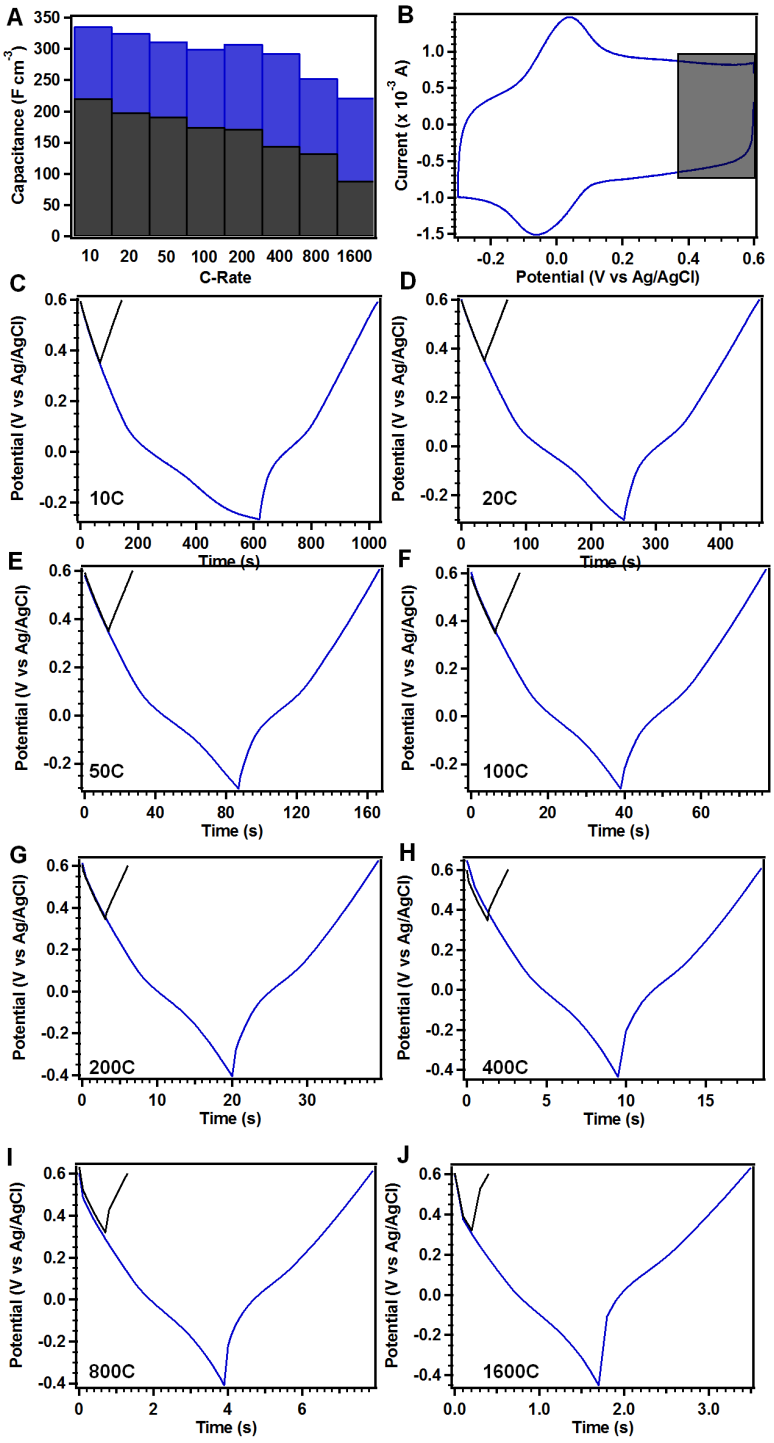

Figure S22. (A) Capacitance over various C rates (x-axis) for PEDOT / **DAAQ-TFP** COF (blue) over the entire voltage window (-0.4 to 0.6 V vs Ag/AgCl) and for PEDOT / **DAAQ-TFP** COF (black) in the non-faradaic window (0.35 – 0.6 V V vs Ag/AgCl). (B) CV of PEDOT / **DAAQ-TFP** COF with the nonfaradaic window used in the analysis highlighted in black. (C-J) GCDC profiles for full window (blue) and nonfaradaic window (black) PEDOT/ **DAAQ-TFP** COF.

Table S2. Percent of capacitance contribution from nonfaradaic region as assessed through the GCDC experiment in Figure S22.

C-rate	Percent nonfaradaic
10	65
20	61
50	61
100	58
200	56
400	49
800	52
1600	40

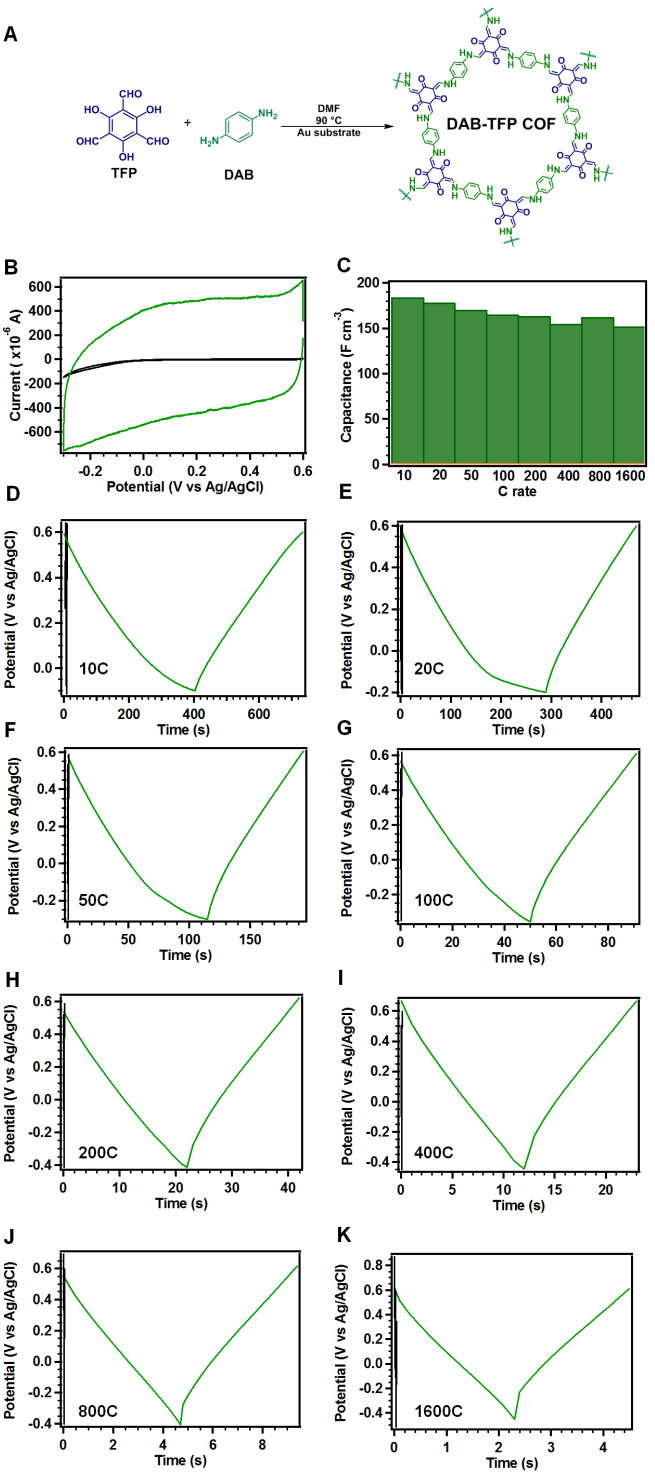

Figure S23. (A) Reaction scheme to synthesize **DAB-TFP** COF film (B) CV of PEDOT / **DAB-TFP** COF (green) and unmodified **DAB-TFP** COF (black). (C) Capacitance over various C rates (x-axis) for PEDOT / **DAB-TFP** COF (green) **DAB-TFP** COF (orange) (D-K) GCDC profiles for PEDOT / **DAB-TFP** COF (green) and **DAB-TFP** COF(black).

Sample calculation for volumetric capacitance

Capacitances were calculated from galvanostatic charge-discharge experiments using the discharge potential-time curve by multiplying the applied current by the discharge time to give A●s then dividing by the potential range and geometric volume of the electrode to give mF cm^{-3}. The applied current was determined by integrating the oxidative half of the cyclic voltammogram of the PEDOT / **DAAQ-TFP** COF film to give charge in mA●s. A rate of 10 C was determined by dividing the charge by 360 s. Each profile shows a voltage plateau around the E_o' of the anthraquinone moieties.

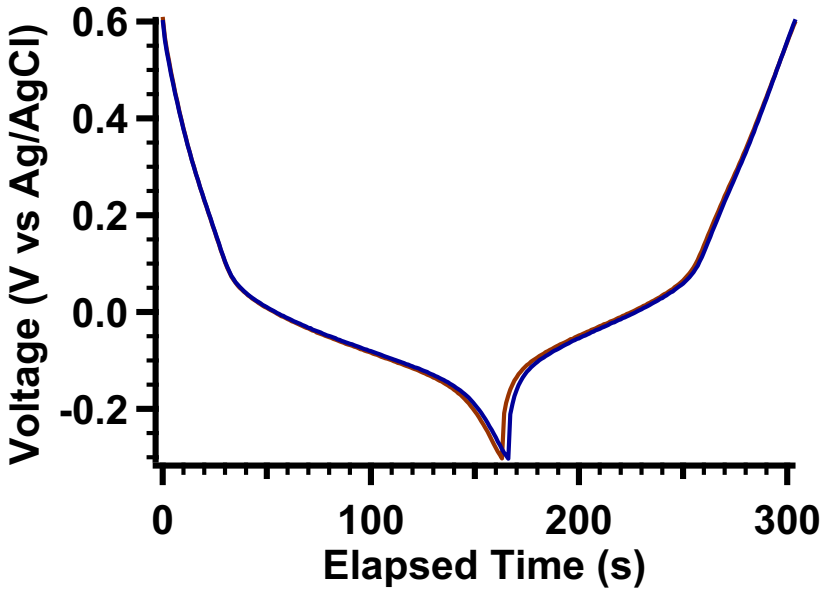

Figure S24. Galvanostatic charge / discharge experiment for PEDOT-modified **DAAQ/TFP** COF film at 50 C. The red trace is cycle 1, the blue trace is cycle 10.

(1) Determine the elapsed time of discharge (oxidation of anthraquinones) Δt = 145 s
(2) Multiply this by the applied current to get charge: 145 s (136 μA) = 0.01972 A●s = 0.01972 C
(3) Divide this by the potential window the oxidation sweep occurs in: 0.01972 C / 0.9 V = 0.022 F

(4) Normalize by the geometric volume for a given film. In this example 1005 nm, which is a volume of 6.4E-5 cm^{-3}: 0.022 F / 6.4E-5 cm^{-3} = 341 F cm^{-3}

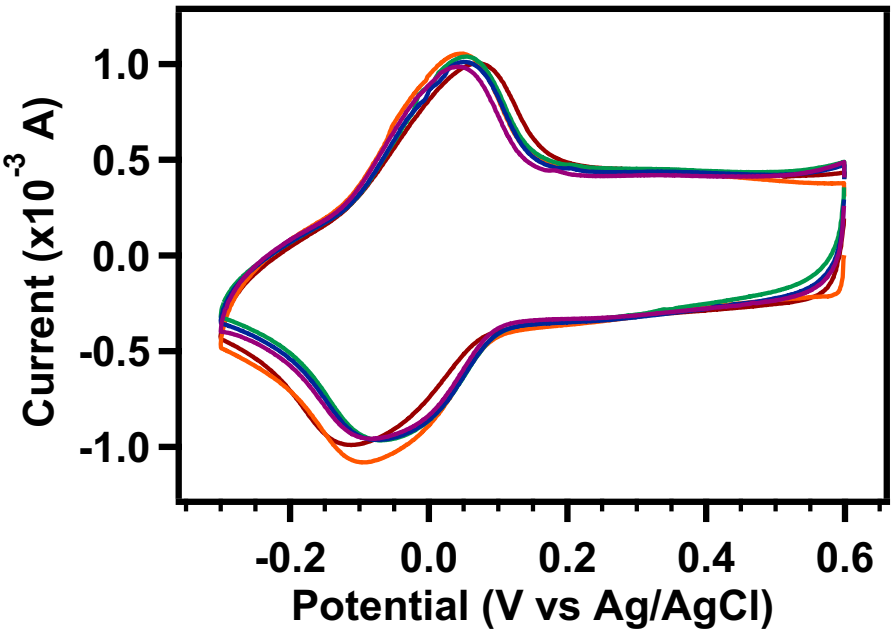

Figure S25. Extended stability test for **DAAQ-TFP** COF / PEDOT after being held at -0.3 V for 15 hours using a potential step experiment. Red trace corresponds to before potential step, orange post 1 h, green post 3 h, blue post 5 h, and purple post 15 h.

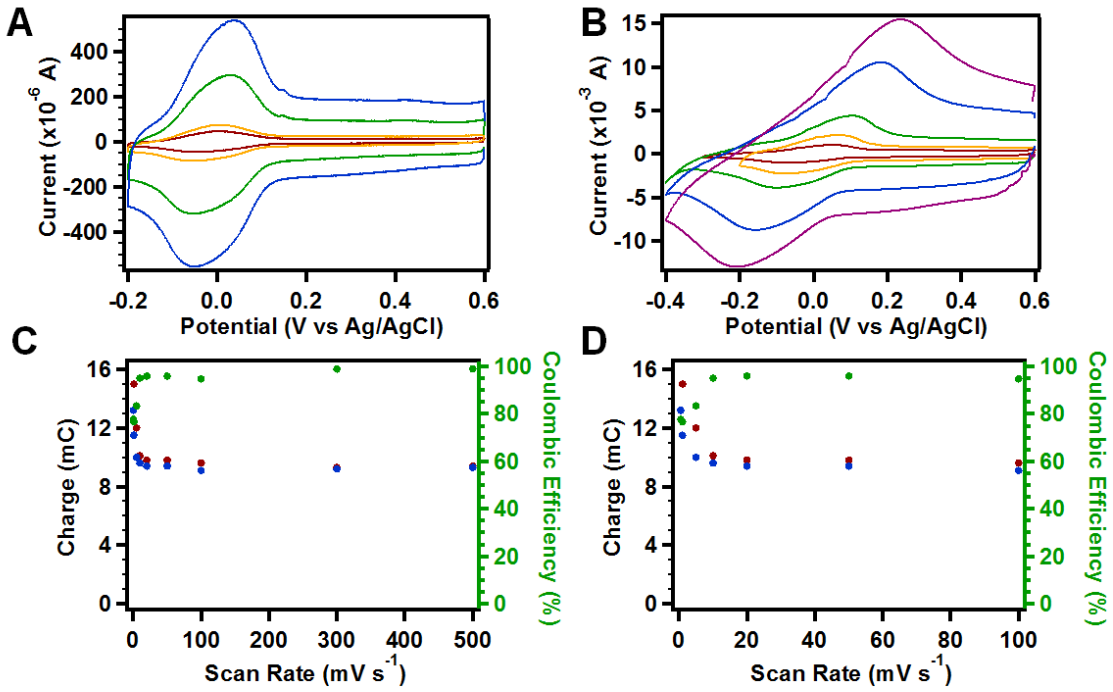

Figure S26. Scan rate dependence experiment at reduced cycling rates. (A) displays the CV response for a PEDOT-modified **DAAQ-TFP** film at 0.5, 1, 5, and 10 mV s^{-1} and (B) for 20, 50, 100, 300, and 500 mV s^{-1}. (C) displays the integrated charge for the oxidative (blue) and reductive (red) anthraquinone waves along with the coulombic efficiency (green, right y-axis) over all scan rates probed in (A) and (B). (D) is a zoom-in of the slowest scan rates shown in part (C).

At very slow sweep rates the coulombic efficiency is less than quantitative, suggesting a form of self-discharge in the system. In order for the PEDOT to access the **DAAQ** groups within the COF, it must be in the doped (conducting) state which was one of the reasons why we chose PEDOT as the electronically conducting polymer in this study. PEDOT's onset potential for doping is negative of the formal potential of the **DAAQ** groups. The onset potential for PEDOT doping depends on a number of variables including solvent and polymer chain length, but it is generally negative of 0.0 V vs Ag/AgCl as is evident in Figure 3 in the manuscript. However, the formal potential for oxidation of the **DAAQ** groups is only slightly positive of the onset of PEDOT doping. Thus, the PEDOT is not fully doped at potentials where **DAAQ** begins to be oxidized. This means that there can be some extent of "operationally" self-discharge especially at very slow sweep rates since the electrode would be effectively "spending more time" in the potential region where these processes would be operative.

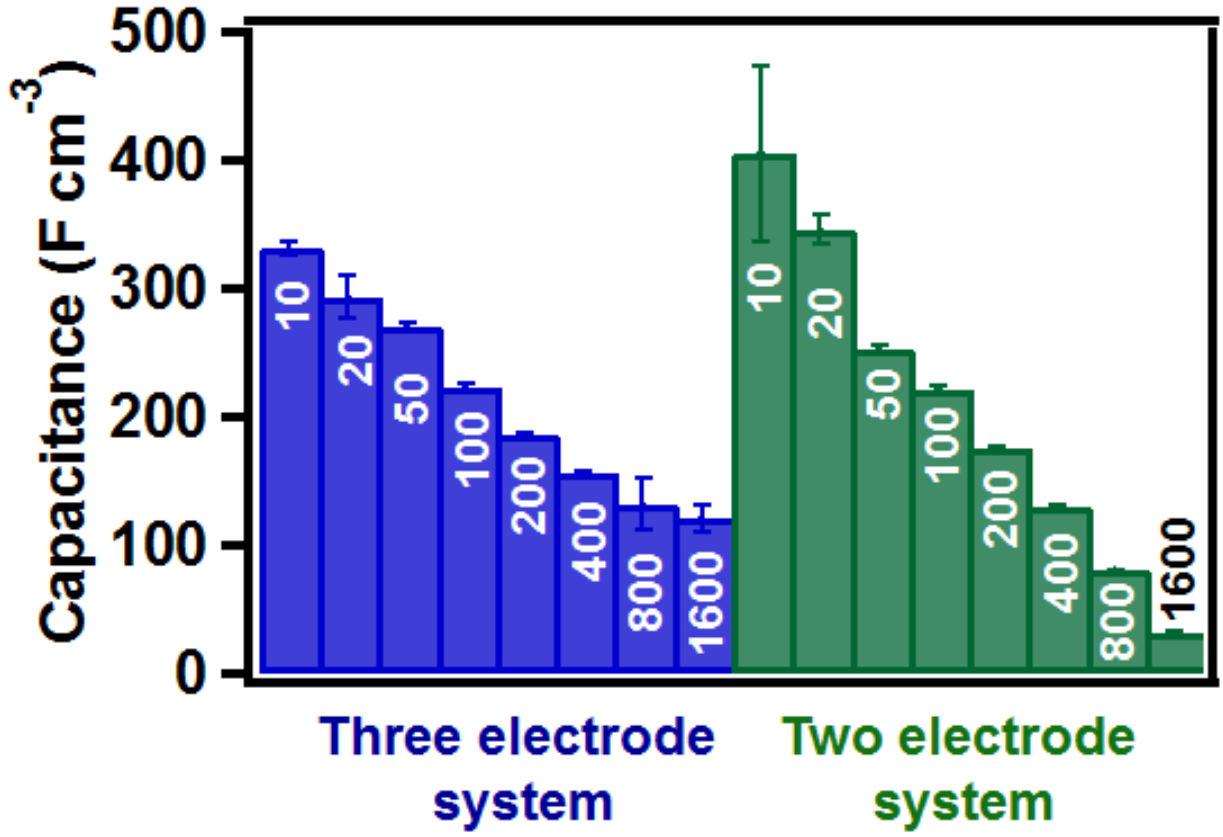

Figure S27. Capacitance responses over a variety of C-rates for three-electrode and two-electrode set up.

Estimation of the mass of a 500 nm thick DAAQ-TFP COF film

(1) Geometric exposed electrochemistry cell area = 0.64 cm^2

(2) Number of unit cells per echem cell:

(i) From the unit cell
Area = 25.8 Å (29.8 Å)
= 770.7 $Å^2$ = 7.7 x 10^{-14} cm^2 per unit cell

(ii) Number of cells = (geometric area of cell) / (area of unit cell)
= (0.64 cm^2) / (7.7 x 10^{-14} cm^2) = 8.3 x 10^{12} unit cells

(iii) Number of moles = 8.3 x 10^{12} unit cells / 6.022 x 10^{23} = 1.4 x 10^{-11} mol

(3) Mass of unit cells in layer:
1026 g mol^{-1} (1.4 x 10^{-11} mol) = 1.4 x 10^{-8} g per layer

(4) Accounting for thickness:
5000 Å / 3.6 Å = 1388 layers
1388 layers (1.4 x 10^{-8} g / layer) = 19 μg

(5) Including PEDOT
11 μg cm^{-2} + 8(20 μg cm^{-2}) = 171 μg cm^{-2}

171 μg cm^{-2}(0.64 cm^2) = 109 μg

Device Preparation/Assembly

*PEDOT modified **DAAQ-TFP** COF powder for coin cell preparation*

The 10:1 and 1:1 PEDOT/COF composites were synthesized *via* chemical oxidation of EDOT in the presence of **DAAQ-TFP** COF powder. A 43 mg portion of EDOT was added into a mixture COF powder (30 mg) in methanol (MeOH) at 0 °C. After 15 minutes of mixing, $Fe(ClO_4)_3$ (0.214 g) was dissolved in MeOH and slowly added to the mixture of COF and EDOT. After stirring for 6 hours, dark blue powder was obtained. The polymer was extensively washed using MeOH to remove traces of $Fe(ClO_4)_3$ and dried at 90 °C overnight.

Coin-shaped electrodes of both cathode (PEDOT/COF) and anode (activated carbon, AC) were prepared by adding 90 mg of material (for cathode, 80 mg of PEDOT/COF + 10 mg Super P carbon, for anode 90 mg of activated carbon) to a scintilation vial that is equipped with a stir bar and 10 mg of polytetrafluoroethylene (PTFE) as a binder. Less than 1 mL of ethanol was added and the mixture was allowed to vigorously mix at 60 °C until the mixture is almost dry. The gels were rolled into a thin film and was allowed to dry at 60 °C overnight.

Cell Assembly and Working

A lithium-ion battery CR2032 cell was used as the device chamber, and was assembled, by stacking a Ti-foil, PEDOT/COF (cathode), separator, activated carbon, Ti-foil, stainless steel, spring and a cap (Figure S28). The diameters of the components may be found in Table S3. CV characterization of single coin cell device was tested by contact using Cu tape. After individual cells were confirmed to be working, two cells were connected in series using Arbin channels connect by wires (Figure S28F). In order to charge a 2.2 V LED, the setup was charged to 2.2 V for 10 s, then was allowed to relax until the LED dimmed completely (about 30 s, see video).

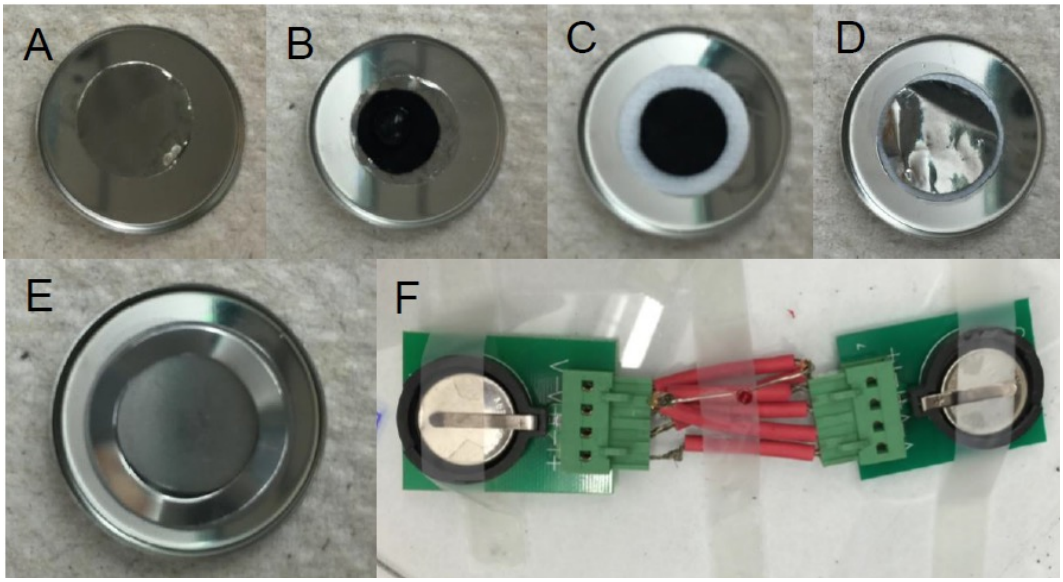

Figure S28. Assembly of a cell. Starting from the cathode, (A) Ti current collector, (B) PEDOT / **DAAQ-TFP** COF, (C) separator and activated carbon, (D) Ti current collector, (E) stainless steel piece and spring, and (F) shows two cell connected in series using Arbin channels connected by wires with the LED attached to the setup.

Table S3. Dimensions of cell components

Component	**Ti current collector**	**PEDOT / DAAQ-TFP COF (1:1)**	**Anode**	**Separator**
Diameter (in)	7/16	5/16	5/16	1/2

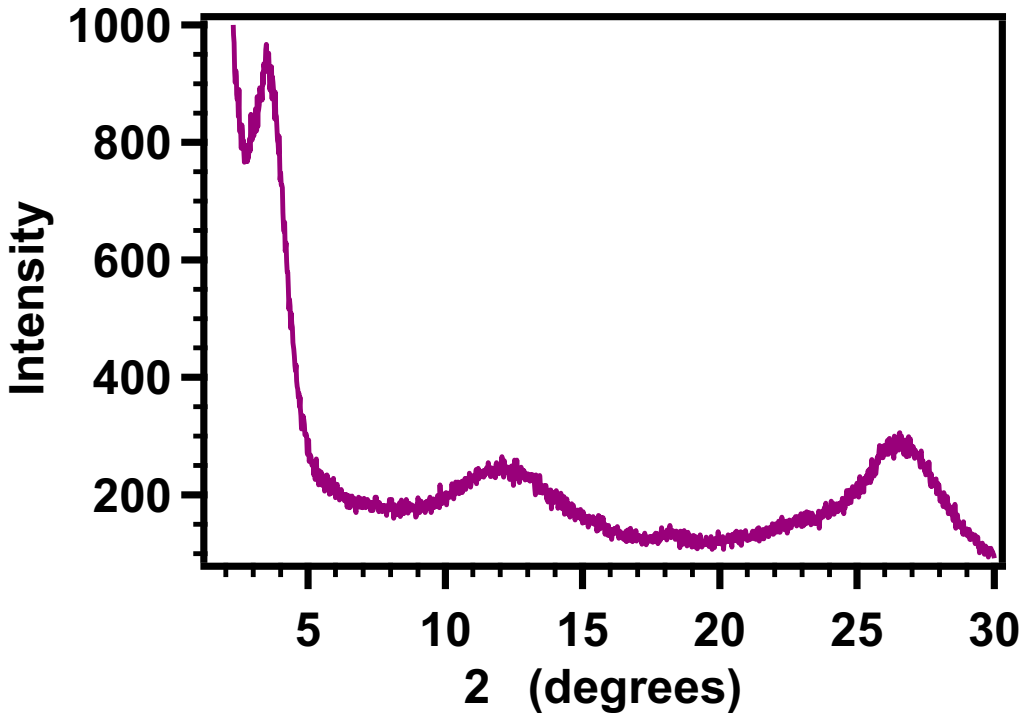

Figure S29. Powder XRD of PEDOT-modified **DAAQ-TFP** powder, showing diffraction pattern maintained.

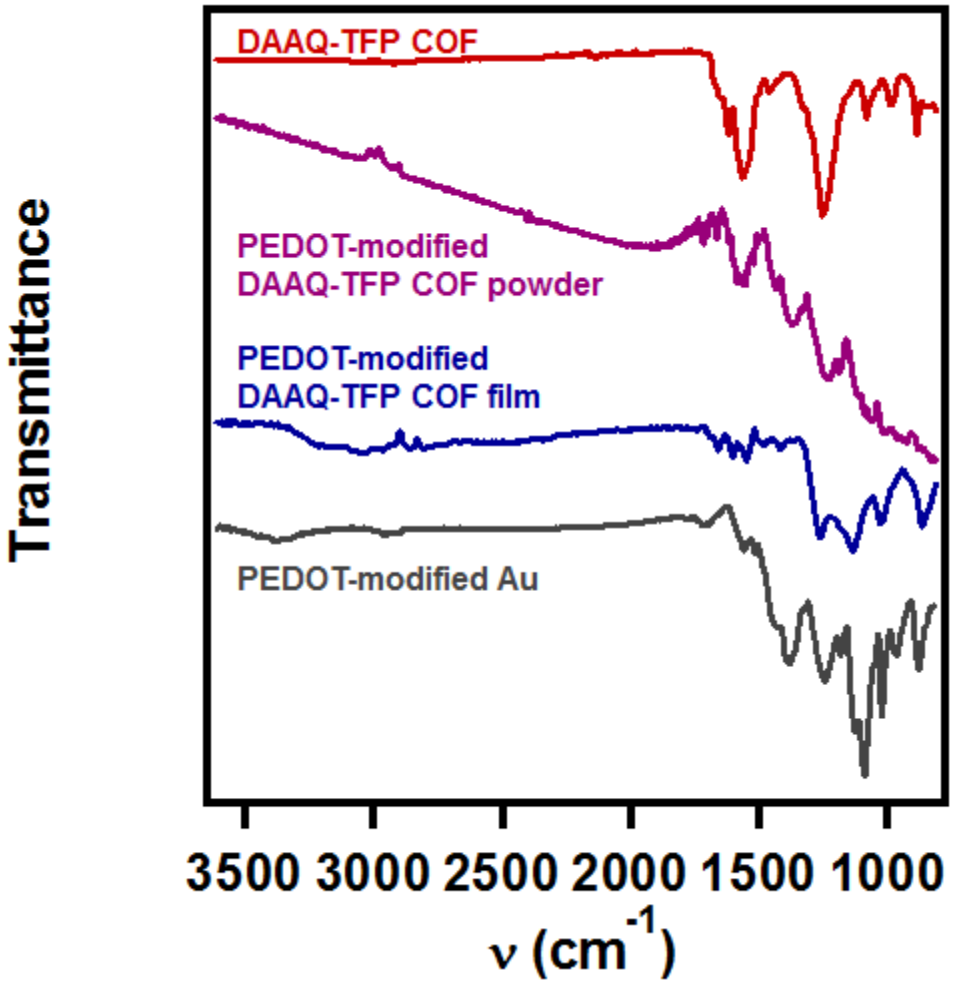

Figure S30. Overlay of IR spectra of **DAAQ-TFP** COF powder (red), chemically polymerized PEDOT-modified **DAAQ-TFP** COF powder (purple), electropolymerized PEDOT-modified **DAAQ-TFP** COF film (blue) and electropolymerized EDOT on Au surface (grey).

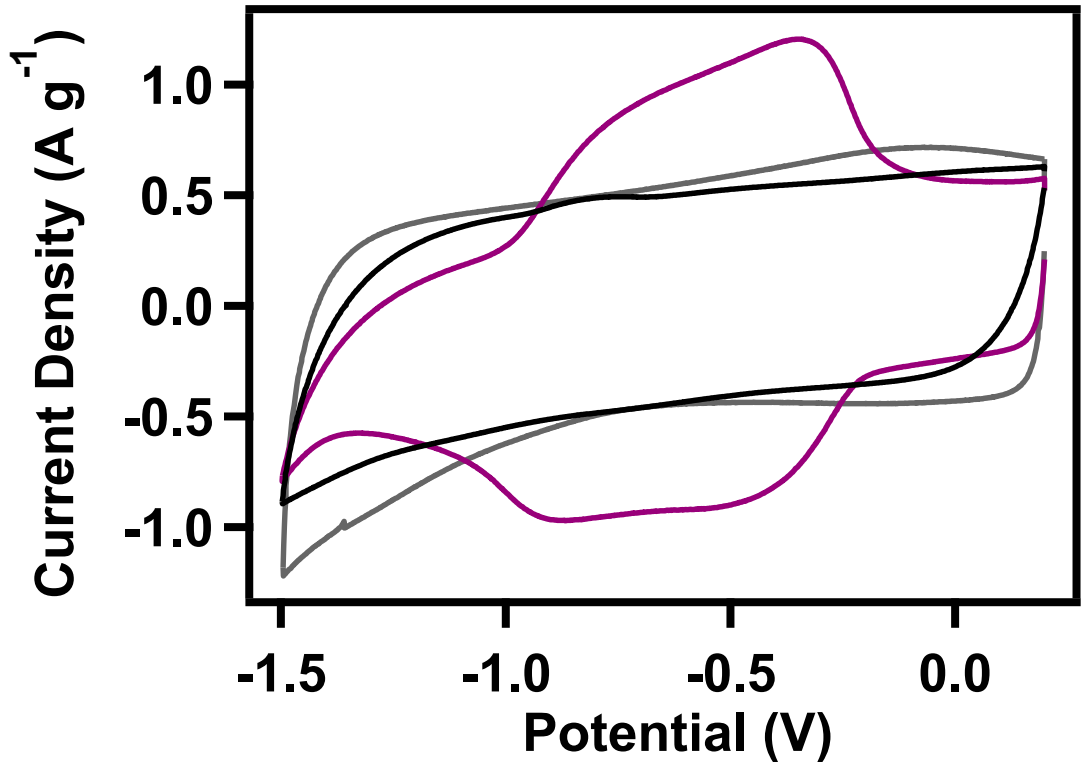

Figure S31. CV response for a coin cell fabricated from PEDOT-modified **DAAQ-TFP** COF powder where the PEDOT to COF mass ratio is 1:1 (purple) and similarly fabricated coin cells with only activated carbon (grey) or with PEDOT only as the active material (black). The mass used in the normalization is the combined active electrode and counter electrode mass.

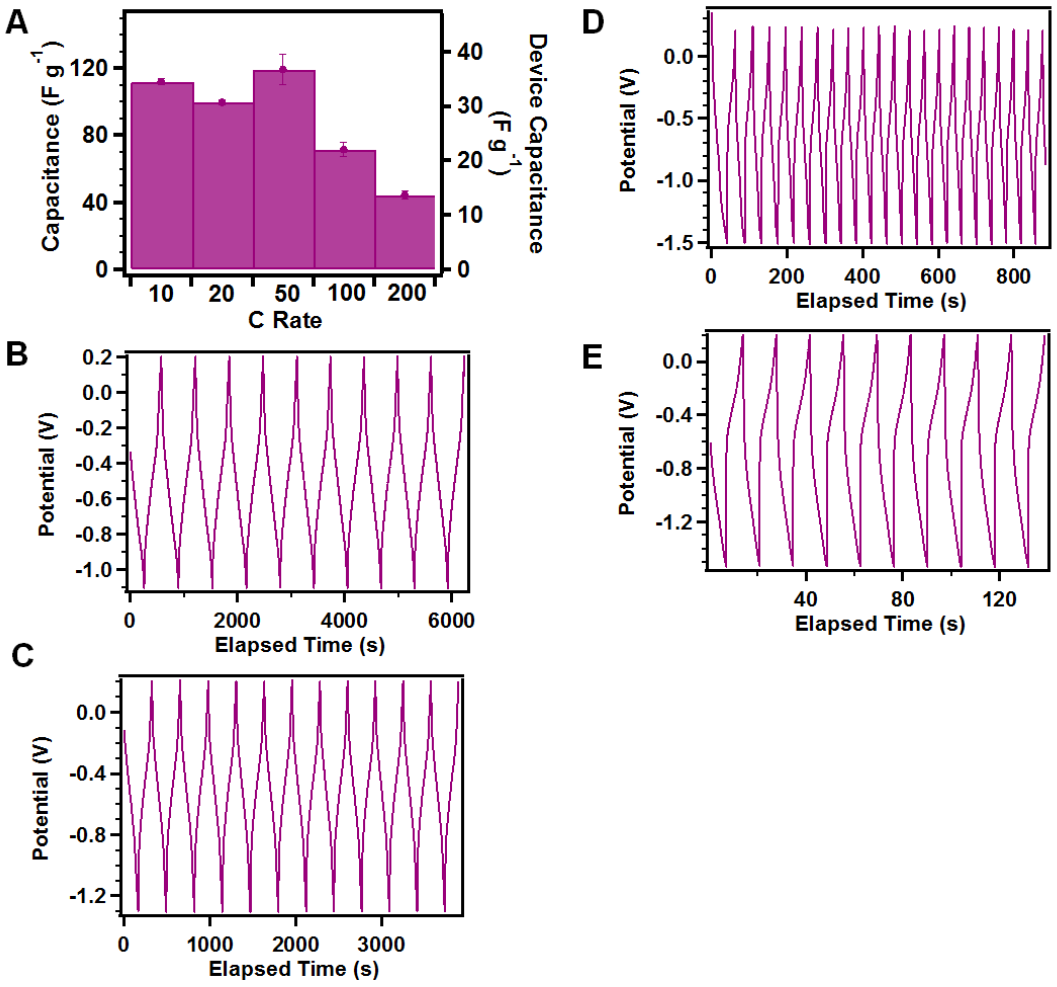

Figure S32. GCDC potential profiles for a coin cell fabricated from PEDOT-modified **DAAQ-TFP** COF powder where the PEDOT to COF mass ration is 1:1 and an activated carbon counter electrode. (A) Capacitance over a variety of C rates where the left axis is the capacitance accounting for the mass of the active electrode only and the right is the capacitance when the whole device is considered. (B) 10C (C) 20C (D) 100C and (E) 200C.

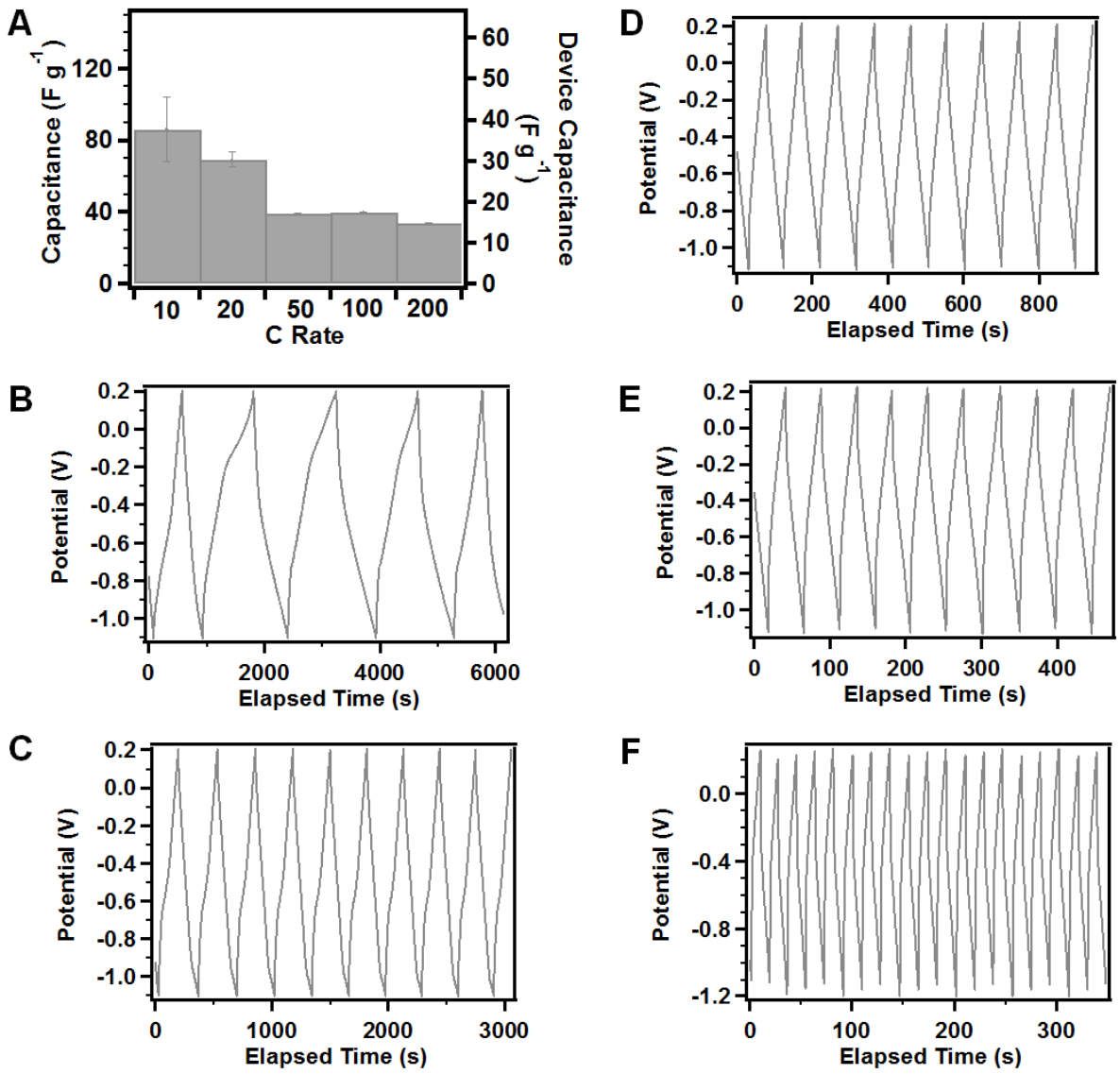

Figure S33. GCDC potential profiles for a coin cell fabricated from PEDOT-only coin cell with activated carbon as counter electrode. (A) Capacitance over a variety of C rates where the left axis is the capacitance accounting for the mass of the active electrode only and the right is the capacitance when the whole device is considered. (B) 10C (C) 20C (D) 50C (E) 100C and (F) 200C.

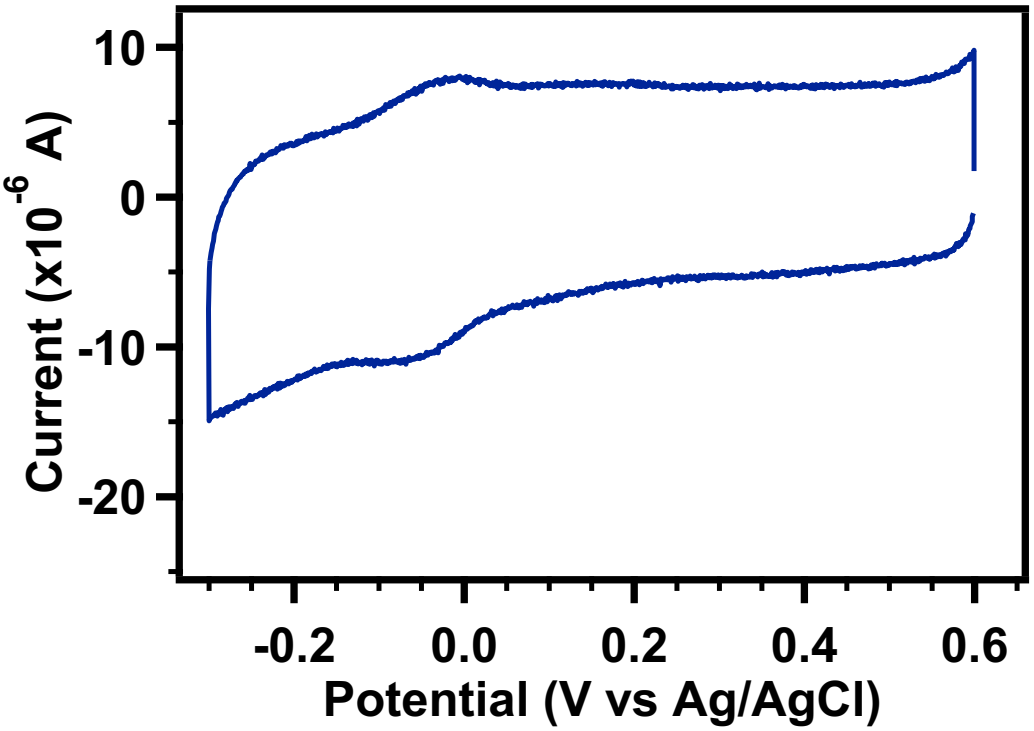

Figure S34. Physical mixture (grinding) of 1-to-1 PEDOT / COF mixture where the PEDOT was chemically polymerized separately from the **DAAQ-TFP** COF powder.

Figure S34 demonstrates that **DAAQ-TFP** COF is physically mixed *via* grinding with PEDOT to prepare a slurry modified electrode similar to our previous preparation,[3] the conducting polymer does not infiltrate the pores and is not intimately mixed with the COF. This CV response provides further support that both the chemical and electrochemical polymerization of EDOT is filling the pores of the **DAAQ-TFP** COF.

I. References

(1) D. M. Smilgies, D. R. Blasini, S. Hotta, H. Yanagi, Reciprocal space mapping and single-crystal scattering rods. *J. Synchrotron Radiat*. **2005**, *12*, 807-811.

(2) Chong, J. H.; Sauer, M.; Patrick, B. O.; MacLachlan, M. J. *Organic letters* **2003**, *5*, 3823–3826.

(3) DeBlase, C. R.; Silberstein, K. E.; Truong, T.; Abruna, H. D.; Dichtel, W. R. Highly Stable Keto-Enamine Salicylideneanilines. *J. Am. Chem. Soc.* **2013**. *135,* 16821–16824.